International Journal of Computer Applications Technology and Research
Volume 7–Issue 07, 241-254, 2018, ISSN:-2319–8656

Hydrocarbon Concentration Levels in Groundwater and Environ, Ethiope West L.G.A. Delta State, N

Ibezue Victoria C (Ph.D)
Department of Geology, Faculty of Physical Sciences, COO University, P.M.B. 02, Uli, Nigeria

Odesa Erhiga G.
Department of Geology, Faculty of Physical Sciences, COO University, P.M.B. 02, Uli, Nigeria

Ndukwe John O
Department of URP, Faculty of Envtl Sciences, COO, University, P.M.B. 02, Uli, Nigeria

Nwa
Depar
A
P
Eb

Abstract

This study investigated Total petroleum hydrocarbon (TPH) content of groundwater samples from Jesse and environs, Delta level of concentration of polycyclic aromatic hydrocarbon and the Aliphatic components in the water sample from the study were collected from ten (10) different water borehole in Urhodo, Okurodo, Ajanasa, Idjedaka. etc in Jesse. The samples colle chromatography method (GC-MS method). The result shows that the polycyclic aromatic hydrocarbon content ranges from aliphatic hydrocarbon content ranges from 0.03 to 0.422 mg/l. This concentrations levels when compared with standa Organization (WHO) tables, indicates that the concentrations of the Total petroleum hydrocarbon is relatively low and with the contamination of the environment by total petroleum hydrocarbon in the study area pose no harmful threat to the env monitoring will serve for the protection of the groundwater supply in the study area. Further oil spillage should be avoided a of hydrocarbons at dangerous level.

Keywords: hydrocarbons, groundwater, concentration, environment, contamination, oil spilla

Introduction

Groundwater contamination resulting from hydrocarbon spill is a major problem in Nigeria. Environmental resource activities; such as industrialization, mining, crude exploitation, that damage water supplies has serious consequences on the ecosystem, this has led to the recognition of its importance, however despite its importance, regulation to prevent and preserve the environment are relatively unsatisfactory in preventing spill to the groundwater. Crude oil is the main source of revenue to the federal government, it contribute over 70% to the foreign earnings of the government [2], and of hydrocarbon, it is made up of a complex mixture of hydrocarbon with different structures and molecular weight, which vary from the highly volatile substance to complex waxes and asphalt components [1].

Hydrocarbons pollution generally pose serious risk to the environment, however, its contribution to the economy and delayed manifestation of effect of oil exploration and exploitation make it difficult to fully appreciate their contribution to the disease burden in Nigeria, especially in the oil-producing communities. The emergence of non-communicable diseases like dermatitis, respiratory difficulties, anaphylactic shock kidney damages, neurological conditions, carcinogenic effects etc [17], among Nigerians has sent a warming message across to stakeholders. Each year, number of Post-Impact Assessment (PIA) studies is conducted

to assess the impact of the hazards genera
physical and social environment and on p
these studies are conducted without any s
health professionals and are reported witho
and long-term implications of the identif
members of the impacted communities [15

Generally, spills and leaks to groundwater,
are potentially dangerous. Hydrocarbons
chains where they disrupt biochemical or pl
organisms, thus causing carcinogenesis in
the genetic material, impairment in reprodu
hemorrhage in exposed population [15]**.**
different definition for pollution comm
introduction into the physical environment
of interfering with human health conditio
natural functioning of the ecosystem (living
surroundings).

Hydrocarbon spillage and fire outbreak in
drew the attention of researchers to the lo
community and its environment. Rese
environmental impact assessment of the r
Little is known about the hydrocarbon cont

in Jesse community and its environment where hydrocarbon spillage has occurred several times. One point is clear that contamination and possible pollution of groundwater by oil spill is significant, dangerous and real in Jesse community and environ.

For water to be adequately utilized, it has to be reasonably free from contaminants. Otherwise, such waters could pose serious health and environmental risks to living organisms that depend on them [5]. The widespread use of petroleum products as fuels, lubricants and solvents has led to high incidence of groundwater contamination by hydrocarbons. Despite the long standing recognition of the pollution threat from petroleum hydrocarbons little has been known about groundwater contamination by these products, as researchers tend to concentrate on the surface environment such as hydrocarbon spillage on surface water and soil.

The objective of the study is to assess and ascertain the level of hydrocarbon concentration in the groundwater of the study area owing to incessant oil spillage. In order to do this, the following steps became necessary; they include:

- To determine the concentrations of hydrocarbon contaminants in groundwater in Jesse town and environs as a result of oil and gas exploration and exploitation activities in the area.
- Evaluate the area extent of the h groundwater in the study area.
- To assess if the groundwater in consistently meet the WHO guidel

Ground elevation in Jesse and environ is above mean sea level and there is a marked rise above the general land scape. The clim with a long wet season lasting from March a short dry season that lasts from Nov temperature average in Jesse is about 27^0C

The study is limited to the confines of a concentrations of hydrocarbon contaminants area as a result of repeated oil spill in Jesse Ethiope West Local Government Area, in D evaluate the impact of hydrocarbon contan Jesse communities and environs using wate sources of groundwater (bore-holes and ha area .The sample was analyzed for Total Pe and PAH using the Gas Chromatography sys

Relevance of the Investigation

This work is relevant to students with interest in water resources and the environment. Water resources and landuse planning experts will borrow a leaf from this study as it provides with vital information on the extent to which human activities can influence the groundwater quality even in the subsurface. Governments and policy makers and in fact all stakeholders in environmental protection and sustainable development will be better advised by consulting this research work. Above all, public health are better secured with adequate and updated information from researches such as this.

Brief Review of Literature

Jesse communities and its environment have been exposed to oil related activities like gas flaring and oil spillage. Gas flares release contaminated fumes into the atmosphere while oil spillage leak oils into the environment either through accidental discharges, sabotage and the likes. When the contaminants get into water bodies, they interfere with the water quality and these could trigger health and environmental effects [3]. However, there have been several approaches developed for the safety and management of environmental impact of oil and natural gas exploration and production operations in the Nigeria. Over the past years, the Nigerian Government has promulgated laws and regulations so that oil and gas exploration and production operations, on oilfields, could be controlled by systems of li the associated environmental impacts.

Some of the related environmental laws and sector include:

*Mineral Oils (safety) R

* Oil in Navigab

* Petroleum Act

* the Federal Agency (FEPA) Act (1

* the National (1989); (revised in 199

* National Envir Limitations), Regulatio Protection (Pollution Generating Wastes) Re

* Environmenta Act (1992), and Depart (DPR) Environmental the Petroleum Industry

The Nigerian situation can be viewed thus: statutory laws and regulations that were intended to provide the framework for Petroleum Resources Exploration and Exploitation did not address issues of petroleum pollution except for a few environmental regulations. Implementation of the laws and regulations are not in view, in spite of the number of existing structures that should have manned that forth of ensuring compliance with rules of operation. Despite all the regulations, groundwater contamination due to petroleum activities is unattended.

Groundwater samples taken from Luiwi in Ogoni land (where oil exploration and exploitation activities have been on till production stopped in 1993) were analyzed in the United State. It was discovered that the sample contained 18ppm of hydrocarbons. This amounts to 360 times the level allowed in drinking water in European Union (E.U) while another sample from Ikwere in Rivers state, Nigeria contained 34ppm and about 680 times the EU standard for drinking water.

The Formation Strata and Groundwater Potential in Sapele Metropolis (which include Jesse and Oghara) was determined by correlating results of seismic refraction survey and those of electrical resistivity studies and discovered that the numbers of layers delineated differ. But the viable aquifer at Sapele and Jesse are generally within 25m below the surface although false and contaminated aquifer may be intercepted at 10 -15 m.

On the contrary, Oghara is more of sandy f
m thick [14].

The ground waters in Warri and Abraka ar
rain and surface water in Okpai and Benel
was examined and the result established th
relatively safe in both cases the rain and su
before it could be consumed [12]

The formation strata and groundwater po
Jesse and Oghara was determined by c
refraction survey and those of electrical
submission was that the numbers of layers d
aquifer at Sapele and Jesse is generally w
although false and contaminated aquifer m
On the contrary, Oghara is more of sandy
35 m thick.

Generally, when petroleum comes in w
between the water, air and sediment part o
[9]. The insoluble fraction forms a layer of
the water layer [10]. During the first few ho
other parts are absorbed in the sediment.
concentrated enough non-aqueous phase liq
The remaining hydrocarbons are present in
on the water surface. The lighter fractions

four hours by evaporation [[13]. However, the evaporation of alkanes is possible until an 18 carbon chain [9]. The mass loss due to evaporation can range for 0.1% for heavier oils to 17.3% for lighter oils [8].

Methodology

The study adopted the experimental research design and used random sampling to select the bore-hole used in the study. Water sample were collected from the selected bore-hole, thereafter the samples were taken to Splendid Stan Research laboratory limited Benin City Nigeria who did the extraction analysis. The method adopted for the sample collection and preparation was in line with America Petroleum Institute (API). Quality assurance /quality control form an integral part of the sample collection processes

By measuring 100 millilitre (100 ± 0.0ml) of water sample, and100 ml of dichloromethane (DCM) via separating funnel and shacked for 30min for BPA extraction. The separating funnel was clamp and the mixture was allowed to separate out. After separation the DCM portion was collected. The process was repeated three times for complete extraction and Gas chromatography analysis was done using Flame Ionization Detection methods. The conditions used were designed to measure the levels of C9 to C36 range of hydrocarbons: An approp program, which separate the solvent peak f the last component, C36, in a reasonable ti was used. Detection was achieved by FID. was computed using statistical model and c in other to determine the significance of the

Findings

The result of the chemical analysis of the from Jesse and environs is presented in the

Table1: Total Aliphatic Hydrocarbon Contents (mg/l)

COMPONENT	Bh1	Bh2	Bh3	Bh4	R1	W1	W2	W3	W4	W5
C8	0.000	0.000	0.000	0.001	0.000	0.004	0.000	0.000	0.000	0.000
C9	0.000	0.000	0.000	0.000	0.000	0.000	0.000	0.000	0.001	0.000
C10	0.000	0.010	0.000	0.000	0.002	0.000	0.020	0.000	0.000	0.000
C11	0.000	0.000	0.000	0.000	0.000	0.000	0.000	0.000	0.000	0.004
C12	0.000	0.000	0.000	0.000	0.000	0.000	0.000	0.100	0.040	0.000
C13	0.010	0.000	0.007	0.005	0.000	0.000	0.000	0.000	0.000	0.000
C14	0.000	0.000	0.000	0.000	0.000	0.000	0.000	0.000	0.000	0.000
C15	0.000	0.000	0.000	0.000	0.000	0.000	0.000	0.000	0.000	0.010
C16	0.000	0.030	0.000	0.010	0.040	0.000	0.000	0.000	0.000	0.000
C17	0.030	0.000	0.000	0.000	0.000	0.020	0.000	0.000	0.000	0.000
Pristane	0.000	0.000	0.000	0.000	0.000	0.000	0.000	0.000	0.000	0.004
C18	0.000	0.000	0.000	0.000	0.000	0.000	0.003	0.000	0.000	0.000
Phytane	0.000	0.000	0.000	0.000	0.000	0.000	0.000	0.000	0.008	0.000
C19	0.000	0.020	0.000	0.000	0.000	0.000	0.000	0.070	0.000	0.040
C20	0.041	0.000	0.000	0.000	0.000	0.000	0.000	0.000	0.000	0.000
C21	0.000	0.000	0.020	0.000	0.000	0.040	0.000	0.000	0.000	0.000
C22	0.010	0.010	0.000	0.020	0.050	0.000	0.030	0.000	0.080	0.000
C23	0.000	0.000	0.000	0.000	0.000	0.000	0.000	0.200	0.000	0.000
C24	0.020	0.000	0.000	0.040	0.000	0.070	0.004	0.000	0.000	0.000
C25	0.000	0.005	0.003	0.000	0.010	0.000	0.000	0.000	0.000	0.000
C26	0.000	0.000	0.000	0.000	0.040	0.000	0.000	0.100	0.005	0.010
C27	0.000	0.000	0.000	0.000	0.000	0.010	0.000	0.000	0.000	0.000
C28	0.000	0.000	0.000	0.000	0.000	0.000	0.000	0.002	0.000	0.000
C29	0.000	0.000	0.000	0.000	0.000	0.000	0.020	0.000	0.003	0.000
C30	0.000	0.000	0.000	0.000	0.000	0.000	0.000	0.000	0.000	0.000
C31	0.000	0.000	0.000	0.000	0.000	0.000	0.000	0.000	0.000	0.000
C32	0.000	0.000	0.000	0.000	0.000	0.000	0.000	0.000	0.000	0.000
C33	0.000	0.000	0.000	0.000	0.000	0.000	0.000	0.000	0.000	0.000
Total(mg/L)	0.081	0.075	0.030	0.076	0.160	0.154	0.077	0.422	0.178	0.058

Total of twenty eight (28) different aliphatic hydrocarbons were tested for across the ten (10) different samples (Bh1, Bh2, B
W4 and W5).

Table 2: Polycyclic Aromatic Hydrocarbon Concentrations in Water Samples (mg/l)

COMPONENT	B h1	B h2	B h3	B h4	R1	W1	W2	W3	W4	W5
Naphthalene	0.000	0.000	0.000	0.000	0.000	0.000	0.000	0.000	0.000	0.0
2-methylinaphthalene	0.000	0.000	0.000	0.000	0.000	0.000	0.000	0.000	0.002	0.0
Acenaphthalene	0.001	0.001	0.001	0.000	0.001	0.000	0.001	0.001	0.000	0.0
Acenaphthene	0.000	0.000	0.002	0.001	0.000	0.00	0.001	0.000	0.001	0.0
Fluorene	0.001	0.000	0.000	0.000	0.000	0.000	0.002	0.001	0.002	0.0
Phenanthrene	0.000	0.000	0.000	0.000	0.001	0.00	0.000	0.000	0.000	0.0
Anthracene	0.001	0.001	0.000	0.001	0.000	0.000	0.000	0.000	0.001	0.0
Fluoranthene	0.000	0.000	0.001	0.000	0.000	0.000	0.000	0.000	0.000	0.0
Pyrene	0.000	0.000	0.000	0.000	0.000	0.000	0.000	0.000	0.000	0.0
Benzo[a]anthracene	0.000	0.000	0.000	0.000	0.000	0.000	0.000	0.000	0.000	0.0
Chrysene	0.000	0.000	0.000	0.000	0.000	0.000	0.000	0.000	0.000	0.0
Benzo[b]fluoranthene	0.000	0.000	0.000	0.000	0.000	0.000	0.000	0.000	0.000	0.0
Benzo[a]pyrene	0.000	0.000	0.000	0.000	0.000	0.000	0.000	0.000	0.000	0.0
Benzo[k]fluoranthene	0.000	0.000	0.000	0.000	0.000	0.000	0.000	0.000	0.000	0.0
Indeno[1,2,3-cd]pyrene	0.000	0.000	0.000	0.000	0.000	0.000	0.000	0.000	0.000	0.0
Dibenzo[a,h]anthracene2	0.000	0.000	0.000	0.000	0.000	0.000	0.000	0.000	0.000	0.0
Benzo[g,h,I]perylene	0.000	0.000	0.000	0.000	0.000	0.000	0.000	0.000	0.000	0.0
Total(mg/L0	0.003	0.002	0.004	0.002	0.002	0.002	0.004	0.002	0.007	0.0

17 different PAHs were tested for in the same sample of groundwater sin the study area. The analytical result of the samples shows the concentrations of the Aromatic components generally fall within the range 0.002-0.007mg/l. The total concentrations of both the Aliphatic and the Aromatic components of the hydrocarbon in the groundwater samples, the concentrations ranges from 0.034mg/l to 0.424mg/l are show in the table below.

Table 3: Summation of concentrations of TPH and PAH in samples

COMPONENT	Bh1	Bh2	Bh3	Bh4	R1	W1	W2	W3	W4	W5
Aliphatics HC	0.081	0.075	0.030	0.076	0.16	0.154	0.077	0.422	0.178	0.05
PAH	0.003	0.002	0.004	0.002	0.002	0.002	0.004	0.002	0.007	0.00
TPH(mg/L)	0.084	0.072	0.034	0.078	0.162	0.156	0.081	0.424	0.185	0.06

The summation of the concentrations are plotted in the bar chart shown below just to show the cor
different sample locations and sources.

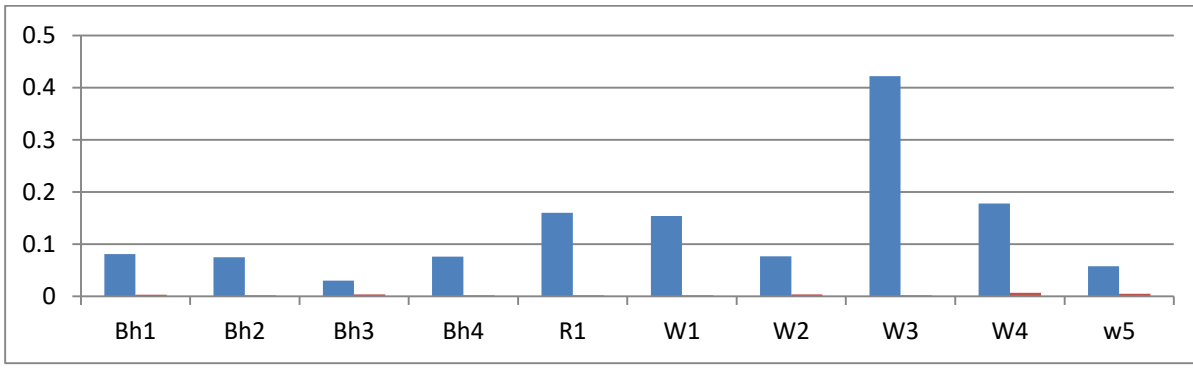

Fig 1: Aromatic and Aliphatic concentration level compared in bar graph (Bh =borehole, W = well)

The chart above shows that the aliphatic components were more in concentration than the aromatics.

The statistical mean compared with the WHO standard of 0.2mg/l reveals that the content of the TPH in the ground water sample is within acceptable limit. T-test analysis on the mean value of hydrocarbon concentrations of groundwater against the acceptable standard as fixed by the world Health Organization (WHO) at 95% significance level, as at the time of study reveals that oil spill in the study area has no significance effect on the groundwater quality, thus the water is suitable for domestic uses and constitute no serious health risk threat.

The aliphatic components were more in concentration than the aromatics. This describes the chemistry of the crude and the fact that the aliphatic seems to persist in groundwater more than the aromatic due to their physical properties which are responsible for the different dispersion rates of the aliphatic and aromatic components. The aromatics are more soluble in nature, this affect the rate of their transportation infiltration and dispersion (transportation). The aliphatic can easily infiltrate through formations to the groundwater due to their less solubility nature, these suggest how fast they travels through the tortious path followed by groundwater which greatly affect the concentration levels; the higher the concentrations of the aliphatic component the more mg/l left in (groundwater).

Only little fractions of aromatic compo petroleum spill in the environment, and t [11]. Other parts are absorbed in the sedin aromatic molecules are soluble in water, or more aromatic rings are not solubl associated with the sediment [4], [15]. Th in sediment and less available in groundw

The rate of mobility for hydrocarbon of th of absorption which tend to concentrates viscosity and high transportation rate of th higher level of the aliphatic component t in groundwater of the study area.

Summary of Findings

The analytical result of the samples sho total petroleum hydrocarbon content in t low, the result of the aliphatic componer 0.03-0.422mg/l while the aromatic com 0.007mg/l.

The analytical result shows that there is little differences in concentrations values of TPH in the samples obtained from the bore-hole and the well, the bore hole values ranges between 0.034-0.084mg/l having the mean value of 0.067mg/l while the samples form the Well ranges from (0.063-0.185) having the mean value of 0.1818 mg/l this little differences in value might be attributed to the result of physical, chemical, and biological effect of the natural remediating factors (biodegradation, sorption, dilution etc.) which might have occurred during the infiltration of the hydrocarbon contaminants. The average borehole depth in Jesse is estimated to be 90ft while the hand dug wells is 48ft. Thus, the differences in depth between the bore-hole and hand dug well allows further microbial activities prior degradation of the hydrocarbon, dilution, sorption etc. which suggest the reason for the changes in the concentration of TPH contents. The values of the sample collected from the surface water (R1) is (0.162) this can also be attributed to the effect of the flowing property of the river such as oxygenation of the water body which enhances easy decomposition of the contaminants.

However, since the study area is made up of over 70% sand, which tend to enhance the mobility and diffusion of the contaminants, the transportation of hydrocarbon contaminants from the point of the spillage to the groundwater must have undergone series of biological, chemical and physical processes that concentrations. Thus, these natural hydrocarbons are therefore considered concentrations of hydrocarbon in the grou

This study was carried out on water sam its environs which underlain by the Benin Basin. The Result of the GC-MS analysis major PAHs; Acenaphthylene, Acenapht and Anthraces and 0.00-0.002mg/l in a locations within the study area. Generall 0.001-0.015mg/l which is within the recommended by WHO in 2012, this infe Hydrocarbon concentrations identified in and as such can pose less threat to the h within the study area

The study however concludes that:

- The level of hydrocarbon conta within acceptable limits
- The petroleum activities in the effect on the groundwater resource

- Groundwater contaminations pose no health risk due to the consumption of the ground water in the study area

This research work centered on identifying the levels of concentration of hydrocarbons in groundwater in the study area with a view to determine the associated risks. It follows however that this research has succeeded in providing vital information as summarized below.

- It reveals the levels of concentration of hydrocarbons in groundwater in Jesse and environs, and the potentials for natural attenuation in the environment.
- The study also tried to bridge the gap in knowledge on the fate of the hydrocarbon spillage and its effect on the groundwater in the study area.
- The study also revealed that the groundwater is safe for domestic usage as long as the trend remained monitored. Monitoring therefore will serve for the protection of the groundwater supply in the study area.

Thus, this study will be of relevance to a wide range of individuals and organizations including; Students and researchers for further studies, government and policy makers and the general public especially the inhabitants of the study area.

References

[1] Abbey, E., Abrams, C. & Athony, N crude oil spillage on soil and microl properties of a tropical rainforest: I studies and biological science Imo 3rded, Pacific Publication : 122-125

[2] Akpofure, A.E., Efere, L.M & Wei, adverse effect of crude oil spill in N Internet web report at http//: www. waado.org/environment.(accessed

[3] Amukali. O. (2012). Effects of gas f water quality for domestic use in Okp State, Nigeria. Unpublished M. Sc. T Geography, University of Maiduguri

[4] Cerniglia, C. E. (1992). Biodegradat hydrocarbons. Biodegradation **3**,351-

[5] Chiyem, F.I., Ohwoghere-Asuma, O 2014). 2D Electrical Resistivity Imag Saturated Zones for crude oil spillage of Delta State, Nigeria: New York Sc

[6] Dami A., Ayuba HK & Amukali O and oil spillage on rainwater collected Beneku, Delta State, Nigeria: Global Jour 12(13),35-45

[7] Dami, A., Ayuba H. K & Amukali, O. (2 in Okpai and Beneku, Ndokwa east loca Nigeria: Journal of Environmental Resear 179.

[8] Delille, D., & Bassères, A. (1998). Influ biodegradation of diesel and crude oil environmental research 45(3), 249-258.

[19] Knap, A. H. (1982). Experimental stu petroleum hydrocarbons from

refinery effluent on an estuarine system: Environmental Science and Technology 16,1-4.

[10] Lichtenthaler, R. G. & Haag, W. R. (1989). Photooxidation of probe compounds sensitized by crude oils in toluene and as an oil film on water: Environmental Science and Technology, 23, 39-45.

[[11] Nicodem, D. E. & Fernandes., M. C. Z. (1997). Photochemical processes and the environmental impact of petroleum spills. Biogeochemistry.2,121-138.

[12] Nwankwo CN & Ogagarue D. O. (2011). Effects of gas glaring on surface and ground waters in Delta State, Nigeria. In Journal of Geology and Mining Research. 3(5), 131-136.

[13] Nwilo, C.P. & Badejo, T.O. (2008). Management of oil dispersal along the Nigerian coastal areas:
Department of Survey & Geoinformatics, University of Lagos, Nigeria. www.oceandocs. org/handle/1834/267

[14] Okolie, Ec; Osemeikhian, Jea & Ujuanbi, O. (2007). Determination of formation strata and groundwater potential in Sapele Metropolis and Environ: Journal of Applied Science and Environmental Management 11(2),181 - 186

[15] Ordinioha B. & Seiyefa B. (2013). The human health implications of crude oil spills in the Niger Delta, Nigeria: an interpretation of published studies: Nigerian Medical Journal, 54:10.

[16] Shor, L. M. & Kosson,. D. S (2004). Combined effects of contaminant desorption and toxicity on risk from PAH contaminated sediments. Risk Analysis,5(2),1109-1120.

[17] United Nation Environment Programme (UNEP 2006). Report on Ogoni-land. Community research and development journal 6(2)101-120.

International Journal of Computer Applications Technology and Research
Volume 7–Issue 07, 255-258, 2018, ISSN:-2319–8656

Prediction of Heart Disease in Diabetic patients using Naive Bayes Classification Technique

Charu V.Verma
Research scholar (CSE)
Dr. C.V. Raman University
Bilaspur, India

Dr. S. M. Ghosh
Professor
Dr. C.V. Raman University
Bilaspur, India

Abstract: The objective of our paper is to predict the risk of heart disease in diabetic patients. In this research paper we are applying Naive Bayes data mining classification technique which is a probabilistic classifier based on Bayes theorem with strong (naive) independence assumptions between the features. Data mining techniques have been widely used in health care systems for prediction of various diseases with accuracy. Health care industry contains large amount of data and hidden information. Effective decisions are made with this hidden information by applying data mining techniques. These techniques are used to discover hidden patterns and relationships from the datasets. The major challenge facing the healthcare industry is the provision for quality services at affordable costs. A quality service implies diagnosing patients correctly and treating them effectively. In this proposed system certain attributes are consider in diabetic patients to predict the risk of heart disease

Keywords: Heart Disease, Diabetes, Data Mining, KDD, Naïve Bayes.

1. INTRODUCTION

The development of Information Technology has generated large amount of databases and huge data in various areas. The area includes health sector, financial sector, weather forecasting, education, manufacturing, fraud detection, bio information etc. The research in databases and information technology has given rise to an approach to store and manipulate this useful data for further decision making. Data mining is the process of discovering patterns in large data bases involving methods at the intersection of machine learning, statistics, and database systems [1]. Popularly data mining referred as knowledge discovery from the data. It is the automated or convenient extraction of patterns representing knowledge implicitly stored or captured in large databases, data warehouses, the Web, other massive information repositories or data streams. The knowledge discovery is an interactive process, consisting by developing an understanding of the application domain, selecting and creating a data set, preprocessing, data transformation.

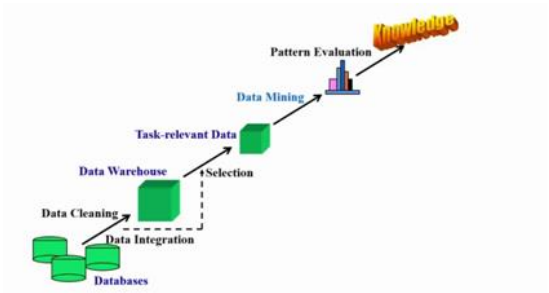

Figure 1: KDD knowledge discovery process

Data mining is the exploration of large datasets to extract hidden and previously unknown patterns, relationships and knowledge that are difficult to detect with traditional statistical methods. Data mining plays a vital role in field of health sector since here huge amounts of data is generated which are too complex and voluminous to be processed and analyzed by traditional methods and difficult to handle manually. Data mining can help healthcare insurers detect fraud and abuse, healthcare organizations make customer relationship management decisions, physicians identify effective treatments and best practices, and patients receive better and more affordable healthcare services. In our busy schedule, most of the people work like a machine in order to live a deluxe and comfortable life in future and to earn more money, but during this type of situation people forget about their health and even don't take any proper rest. Because of this they affected from various type of diseases at a very early age, which cause our health as Diabetes, Heart Disease, Cancer, Eyes, Kidney failure and many more.

Diabetes Mellitus (DM) is commonly referred as Diabetes; it is the condition in which the body does not properly process food for use as energy. Most of the food we eat is turned into glucose or sugar for energy. The pancreas, an organ makes a hormone called insulin to help glucose get into the cells of our bodies. When a body is affected with diabetes, it couldn't make enough insulin or couldn't use its own insulin. This causes sugar to build up into blood. Several pathogenic processes are involved in the development of diabetes. These range from autoimmune destruction of the β-cells of the pancreas with consequent insulin deficiency to abnormalities that result in resistance to insulin action. Diabetes is a life threatening disease in rural and urban, then developed and under developed countries. The common symptoms for the diabetic patients are frequent urination, increased thirst, weight loss, slow-healing in wound, giddiness, increased hunger etc. Diabetes can cause serious health complications including heart disease, blindness, kidney failure and low-extremity amputations.

Types of Diabetes

Type 1Diabetes is called insulin-dependent diabetes mellitus (IDDM) or juvenile-onset diabetes. Autoimmune, genetic, and environmental factors are involved in the development of this type of diabetes. Type1 mostly occurs in young people who

are below 30 years. This type can affect children or adults, but majority of these diabetes cases were in children. In persons with type 1 diabetes, the beta cells of the pancreas, which are responsible for insulin production, are destroyed due to autoimmune system.

Type 2 Diabetes is called non-insulin-dependent diabetes mellitus (NIDDM) or adult-onset diabetes. In the type 2 diabetes, the pancreas usually produces some insulin the amount produced is not enough for the body's needs, or the body's cells are resistant to it. Risk factors for Type 2 diabetes includes older age, obesity, family history of diabetes, prior history of gestational diabetes, impaired glucose tolerance, physical inactivity, and race/ethnicity.

Gestational Diabetes is the third main form and occurs when pregnant women without a previous history of diabetes develop a high blood glucose level. The majority of gestational diabetes patients can control their diabetes with exercise and diet. In such cases between 10%-20% of them will need to take some kind of blood-glucose-controlling medications. In few cases this gestational diabetes may lead to type 2 diabetes in future. It affects on 4% of all pregnant women [2].

Heart disease is the leading cause of death in the world over the past 10 years. Researchers have been using several data mining techniques in the diagnosis of heart disease. Heart diseases are the number 1 cause of death globally: more people die annually from heart disease than from any other cause. An estimated 17.7 million people died from heart disease in 2015, representing 31% of all global deaths. Of these deaths, an estimated 7.4 million were due to coronary heart disease and 6.7 million were due to stroke. Over three quarters of heart disease deaths take place in low- and middle-income countries. Out of the 17 million premature deaths (under the age of 70) due to non communicable diseases in 2015, 82% are in low- and middle-income countries, and 37% are caused by this disease. People with cardiovascular disease or who are at high cardiovascular risk (due to the presence of one or more risk factors such as hypertension, diabetes, hyperlipidaemia or already established disease) need early detection and management using counseling and medicines, as appropriate [3]. Now a day's heart disease is a major health problem and cause of death all over the world. Heart is a very valuable part of our body, and plays a very important role in our life. Our whole life depends on efficient working of heart. The most important behavioral risk factors of heart disease and stroke are unhealthy diet, physical inactivity, tobacco use and harmful use of alcohol. The effects of behavioral risk factors may show up in individuals as raised blood pressure, raised blood glucose, raised blood lipids, and overweight and obesity. These "intermediate risks factors" can be measured in primary care facilities and indicate an increased risk of developing a heart attack, stroke, heart failure and other complications.

Heart disease is caused due to narrowing or blockage of coronary arteries. This is caused by deposition of fat on inner walls of arteries and also due to build up cholesterol. There are some of major heart disease factors which include Diabetes, high blood pressure, high cholesterol, obesity, family history, smoking, eating habits, alcohol that affects our whole body.

2. METHODOLOGY APPLIED

DATA MINING in health care has become increasingly popular because it can improved our patient care by early detecting of disease supports helping care providers for treatment programs and reduces the cost of health care. [4]

Data Mining is major anxious with the study of data and Data Mining tools and techniques are used for discovery patterns from the data set. The most important aim of Data Mining is to find patterns mechanically with least user input and efforts. Data Mining is an influential tool able of usage decision building and for forecasting expectations trends of market. Data Mining tools and techniques can be effectively functional in different fields in different forms. Many Organizations now begin using Data Mining as a tool, to contract with the aggressive surroundings for data analysis. By using Mining tools and techniques, different fields of business get advantage by simply assess various trends and pattern of market and to make rapid and efficient market trend analysis. Data mining is very helpful tool for the diagnosis of diseases.

Classification Technique

Classification derives a model to determine the class of an object based on its attributes. A collection of records will be available, each record with a set of attributes. One of the attributes will be class attribute and the goal of classification task is assigning a class attribute to new set of records as accurately as possible. Mainly classification is used to classify every item in a set of data into one of predefined set of classes or groups.

Naïve bayes is one of technique of classification used for prediction of data. Naive Bayes classifiers is a probabilistic classifiers based on applying Bayes' theorem with strong (naive) independence assumptions between the predictors. A Naive Bayesian model is easy to build, with no complicated iterative parameter estimation which makes it particularly useful for large datasets such as in the field of medical science for diagnosing heart patients. Despite its simplicity, the Naive Bayesian classifier often does surprisingly well and is widely used because it often outperforms more sophisticated classification methods [8]. Bayes theorem provides a way of calculating the posterior probability, P(c|x), from P(c), P(x), and P(x|c). Naive Bayes classifier assumes that the effect of the value of a predictor (x) on a given class (c) is independent of the values of other predictors. This assumption is called class conditional independence.

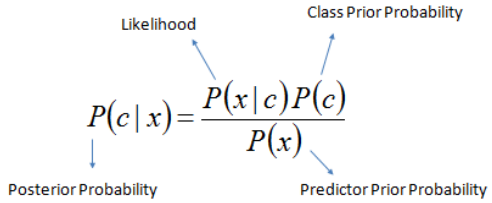

$$P(c \mid X) = P(x_1 \mid c) \times P(x_2 \mid c) \times \cdots \times P(x_n \mid c) \times P(c)$$

2.1 Equations:

• P(c|x) is the posterior probability of class (target) given predictor (attribute).

• P(c) is the prior probability of class.

• P(x|c) is the likelihood which is the probability of predictor given class.

• P(x) is the prior probability of predictor Where C and X are two events. Where C and X are two events. Such Naive Bayes model is easy to build and particularly useful for very large data sets. Along with simplicity, Naive Bayes is known to outperform even highly sophisticated classification methods [4].

2.2 Processing Data set

The patient data set is compiled from UCI data repositories as combined data from Statlog data set and Cleveland Clinic Foundation for heart patients. Here we are taken 14 attributes with nominal values from the database that are considered for the required prediction they are age, sex, chest pain(cp), Blood Pressure(trestbsp), diabetes(fbs)(its value is always 1), ECG(restecg), Heart Rate(thalach), exang, oldpeak, slope, thal, blood Cholesterol(chol) and num (heart disease diagnosis). Where if the num value is present then there is presence of heart disease and if the num value is absent then no heart disease.

2.3 Tool used

Waikato Environment for Knowledge Analysis (WEKA) has been used for prediction due to its proficiency in discovering, analysis and predicting patterns. It was developed at the University of Waikato in New Zealand and easiest way to use is through a graphical user interface called Explorer. Weka is a collection of machine learning algorithms for data mining tasks, written in Java and contains tools for data pre-processing, classification, regression, clustering, association rules, and visualization

2.4 10 fold cross validation

Cross-validation, a standard evaluation technique, is a systematic way of running repeated percentage splits. Cross-validation is a technique to evaluate predictive models by partitioning the original sample into a training set to train the model, and a test set to evaluate it. In k-fold cross-validation, the original sample is randomly partitioned into k equal size subsamples. Of the k subsamples, a single subsample is retained as the validation data for testing the model, and the remaining k-1 subsamples are used as training data. The cross-validation process is then repeated k times (the folds), with each of the k subsamples used exactly once as the validation data. The k results from the folds can then be averaged (or otherwise combined) to produce a single estimation. The advantage of this method is that all observations are used for both training and validation, and each observation is used for validation exactly once[7]. Divide a dataset into 10 pieces (“folds”), then hold out each piece in turn for testing and train on the remaining 9 together. This gives 10 evaluation results, which are averaged. In “stratified” cross-validation, when doing the initial division we ensure that each fold contains approximately the correct proportion of the class values. Having done 10-fold cross-validation and computed the evaluation results, Weka invokes the learning algorithm a final (11th) time on the entire dataset to obtain the model that it prints out [6].

We will simply define and calculate the accuracy, sensitivity, and specificity from the confusion matrix.

True positive (TP) = the number of cases correctly identified as patient

False positive (FP) = the number of cases incorrectly identified as patient

True negative (TN) = the number of cases correctly identified as healthy

False negative (FN) = the number of cases incorrectly identified as healthy

Accuracy: The accuracy of a test is its ability to differentiate the patient and healthy cases correctly. To estimate the accuracy of a test, we should calculate the proportion of true positive and true negative in all evaluated cases. Mathematically, this can be stated as:

Accuracy= (TP+TN)/TP+TN+FP+FN

Sensitivity: The sensitivity of a test is its ability to determine the patient cases correctly. To estimate it, we should calculate the proportion of true positive in patient cases. Mathematically, this can be stated as:

Sensitivity=TP/TP+FN

Specificity: The specificity of a test is its ability to determine the healthy cases correctly. To estimate it, we should calculate the proportion of true negative in healthy cases. Mathematically, this can be stated as:

Specificity=TN/TN+FP

3. EXPERIMENTAL RESULT

The result in our experiment is given of heart disease in diabetic patients. In our experiment we had proposed Naive bayes classification technique as experimental result shown in the figure 2. Accuracy, Sensitivity, Specificity has been calculated from the both confusion matrix of both the performed experiments. For heart disease model accuracy is 89.41%, Sensitivity is 46.05%, Specificity is 55.55%

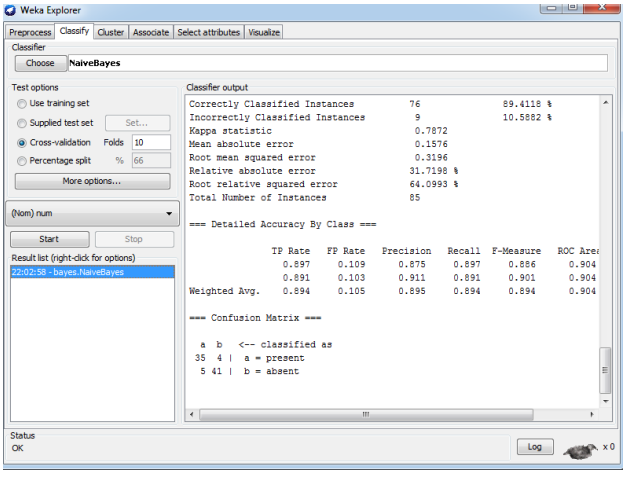

Figure 2 Result window of heart disease data set having Diabetes

Table 1. Result of detailed accuracy class of diabetes patient having heart disease

	Tp	Fp	Pre	Recall	Fm	ROC

Heart disease with diabetes	0.894	0.105	0.895	0.894	0.894	0.904

4. CONCLUSION

In this research paper application of data mining is used to analyze the clinical dataset to detect diseases and diagnosis based on the data and the attributes provided. In the proposed works Naive Bayes classification technique helps to predict heart disease in diabetic patient. From the system we get confusion matrix from which we can predict accuracy of the applied Naïve Bayes algorithm. The result shows that accuracy of our applied algorithm is 89.41% in the prediction of risk of heart disease in diabetic patient. As a future work, further data analysis has been planned to perform other data mining algorithms to improve the classification accuracy.

5. REFERENCES

[1] https://en.wikipedia.org/wiki/Data_mining

[2] http://www.who.int/news-room/fact-sheets/detail/cardiovascular-diseases-(cvds)

[3] https://www.researchgate.net/publication/312188365 ”Heart Attack prediction using Data mining technique”

[4] https://www.analyticsvidhya.com/blog/2017/09/naive-bayes-explained/

[5] https://www.futurelearn.com/courses/data-mining-with-weka/0/steps/25384.

[6] https://www.openml.org/a/estimation-procedures/1

[7] http://www.saedsayad.com/naive_bayesian.htm

[8] https://www.ncbi.nlm.nih.gov/pmc/articles/PMC4614595

International Journal of Computer Applications Technology and Research
Volume 7–Issue 07, 259-269, 2018, ISSN:-2319–8656

Decay Property for Solutions to Plate Type Equations with Variable Coefficients

Shikuan Mao
School of Mathematics and Physics,
North China Electric Power University,
Beijing 102206, China

Xiaolu Li
School of Mathematics and Physics,
North China Electric Power University,
Beijing 102206, China

Abstract: In this paper we consider the initial value problem for a plate type equation with variable coefficients and memory in $\mathbb{R}^n\ (n\geq 1)$), which is of regularity-loss property. By using spectrally resolution, we study the pointwise estimates in the spectral space of the fundamental solution to the corresponding linear problem. Appealing to this pointwise estimates, we obtain the global existence and the decay estimates of solutions to the semilinear problem by employing the fixed point theorem.

Keywords: plate equation, memory, decay, regularity-loss property.

1. INTRODUCTION

In this paper we consider the following initial value problem for a plate type equation in $\mathbb{R}^n\ (n\geq 1)$:

$$\begin{cases}\left(1-\Delta_g\right)u_{tt}+\left(1+\Delta_g^2\right)u+\alpha u_t+\beta k*\left(-\Delta_g\right)^p u_t=f\left(u,u_t,\nabla u\right) \\ u\left(x,0\right)=u_0\left(x\right),u_t\left(x,0\right)=u_1\left(x\right)\end{cases} \quad (1.1)$$

Here $0\leq p\leq 2$, $\alpha>0,\beta>0$ are real numbers, the subscript t in u_t and u_{tt} denotes the time derivative (i.e., $u_t=\partial_t u, u_{tt}=\partial_t^2 u$),

$\Delta_g=\frac{1}{\sqrt{G}}\sum_{ij=1}^n \partial_{x_i}\sqrt{G}g^{ij}\partial_{x_j}$ is the Laplace(-Beltrami) operator associated with the Riemannian metric

$$g=\sum_{ij=1}^n g_{ij}\left(x\right)dx_i\otimes dx_j,\ G=\left|\det\left(g_{ij}\right)\right|$$

and $\left(g^{ij}\right)=\left(g_{ij}\right)^{-1}$, $u=u\left(x,t\right)$ is the unknown function of $x\in R^n$ and $t>0$, and represents the transversal displacement of the plate at the point x and t, $\Delta_g u_{tt}$ corresponds to the rotational inertial. The term u_t represents a frictional dissipation to the plate. The term

$$k*\left(-\Delta_g\right)^p u_t:=\int_0^t k\left(t-\tau\right)\left(-\Delta_g\right)^p u_t\left(\tau\right)d\tau$$

corresponds to the memory term, and $k\left(t\right)$ satisfies the following assumptions:

Assumption [A]. $k\in C^2\left(R^+\right)$, $k\left(s\right)>0$, and the derivatives of k satisfy the following conditions

$$-C_0k\left(s\right)\leq k'\left(s\right)\leq -C_1k\left(s\right),$$

$$C_2k\left(s\right)\leq k''\left(s\right)\leq C_3k\left(s\right),\forall s\in\left(R^+\right).$$

Where $C_i\ (i=0,1,2,3)$ are positive constants.

We suppose the metric g satisfies the following conditions:

Assumption [B]. The matrix g^{ij} is symmetric for each $x\in\mathbb{R}^n$, and there exists $C_\alpha>0$ and $C>0$ such that

$(i)\ g^{ij}\in C^\infty\left(\mathbb{R}^n\right),\left|\partial_x^\alpha g^{ij}\left(x\right)\right|\leq C_\alpha$,

$\forall x\in\mathbb{R}^n,\alpha\in\mathbb{R}_+^n$.

$(ii)\ C_1\left|\xi\right|^2\leq\sum_{ij=1}^n g^{ij}\left(x\right)\xi_i\xi_j\leq C_2\left|\xi\right|^2$,

$\forall x\in\mathbb{R}^n,\forall\xi\in\mathbb{R}^n$.

Assumption [C]. $f\in C^\infty\left(\mathbb{R}^{n+2}\right)$ and there exists $\eta\in\mathbb{R}^+$ satisfying $\eta>1$ such that $f\left(U\right)=O\left(\left|U\right|^\eta\right)$, as $\left|U\right|\to 0$.

It is well known that under the above assumptions, the Laplace operator Δ_g is essentially self-adjoint on the Hilbert space $H=L^2\left(\mathbb{R}^n,d\mu_g\right)$ with domain $C_0^\infty\left(\mathbb{R}^n\right)$, here $d\mu_g=\sqrt{G}dx$. We denote the unique self-adjoint extension (to the Sobolev space $H^2\left(\mathbb{R}^n\right)$) by the same symbol Δ_g. The spectrum of $-\Delta_g$ is $\left[0,+\infty\right)$, and it generates a contraction semi-group $e^{t\Delta_g}$ on $L^p\left(\mathbb{R}^n\right)$

$(1 \le p \le \infty)$, We note by our assumptions of the metric g, the measure $d\mu_g$ is equivalent to dx, and by the (functional) calculus for pseudodifferential operators, we have the following classical equivalence (cf. [8, 5]): For $s \in \mathbb{R}$, there exists $C_s > 0$, such that

$$C_s^{-1}\|u\|_{H^s} \le \left(u, (1-\Delta_g)^{\frac{s}{2}} u\right)_{L^2} \le C_s \|u\|_{H^s} \quad \forall u \in S(\mathbb{R}^n) \qquad (1.2)$$

where $S(\mathbb{R}^n)$ is the class of Schwartz functions.

The main purpose of this paper is to study the global existence and decay estimates of solutions to the initial value problem (1.1). For our problem, it is difficult to obtain explicitly the solution operators or their Fourier transform due to the presence of the memory term and variable coefficients. However, we can obtain the pointwise estimate in the spectral space of the fundamental solution operators to the corresponding linear equation

$$(1-\Delta_g)u_{tt} + (1+\Delta_g^2)u + \alpha u_t + \beta k * (-\Delta_g)^p u_t = 0 \qquad (1.3)$$

from which the global existence and the decay estimates of solutions to the semilinear problem can be obtained. The following are our main theorems.

Theorem 1.1 (energy estimate for linear problem). Let $s > 0$ be a real number. Assume that $u_0 \in H^{s+\max\{1,2p-2\}}(\mathbb{R}^n)$ and $u_1 \in H^s(\mathbb{R}^n)$, and put

$$I_0 = \|u_0\|_{H^{s+\max\{1,2p-2\}}} + \|u_1\|_{H^s}.$$

Then the solution to the problem (1.3) with initial condition $u(0) = u_0$ and $u_t(0) = u_1$ satisfies

$$u \in C^0\left([0,\infty); H^{s+1}(\mathbb{R}^n)\right) \cap C^1\left([0,\infty); H^s(\mathbb{R}^n)\right)$$

and the following energy estimate:

$$\|u(t)\|_{H^{s+1}}^2 + \|u_t(t)\|_{H^s}^2 + \int_0^t \left(\|u(\tau)\|_{H^s}^2 + \|u_t(\tau)\|_{H^{s-1}}^2\right) d\tau \le CI_0^2.$$

The second one is about the decay estimates for the solution to (1.3), which is stated as follows:

Theorem 1.2 (decay estimates for linear problem). Under the same assumptions as in Theorem 1.1, then the solution to (1.3) satisfies the following decay estimates:

$$\|u(t)\|_{H^{s+1-\sigma}} \le CI_0(1+t)^{-\frac{\sigma}{2}},$$

for $0 \le \sigma \le s+1$, and

$$\|u_t(t)\|_{H^{s-\sigma}} \le CI_0(1+t)^{-\frac{\sigma}{2}},$$

for $0 \le \sigma \le s$.

Theorem 1.3 (existence and decay estimates for semilinear problem). Let $s > \frac{n}{2}$ and $0 \le p \le 2$ be real numbers. Assume that $u_0 \in H^{S+\max\{1,2p-2\}}(\mathbb{R}^n)$, $u_1 \in H^s(\mathbb{R}^n)$, and put

$$I_0 = \|u_0\|_{H^{s+\max\{1,2p-2\}}} + \|u_1\|_{H^s}$$

then there exists a small $\varepsilon > 0$, such that when $I_0 \le \varepsilon$, there exists a unique solution to (1.1) in

$$u \in C^0\left([0,\infty); H^{s+1}(\mathbb{R}^n)\right) \cap C^1\left([0,\infty); H^s(\mathbb{R}^n)\right)$$

satisfying the following decay estimates:

$$\|u(t)\|_{H^{s+1-\sigma}} \le CI_0(1+t)^{-\frac{\sigma}{2}}, \qquad (1.4)$$

for $0 \le \sigma \le s+1$, and

$$\|u_t(t)\|_{H^{s-\sigma}} \le CI_0(1+t)^{-\frac{\sigma}{2}}, \qquad (1.5)$$

for $0 \le \sigma \le s$.

Remark 1. If the semilinear term is the form of $f(u)$, then we may assume $s > 0 (n=1)$ and $s+1 \ge \frac{n}{2} (n \ge 2)$ in Theorem 1.3.

For the study of plate type equations, there are many results in the literatures. In [4], da Luz–Charão studied a semilinear damped plate equation :

$$u_{tt} - \Delta u_{tt} + \Delta^2 u + u_t = f(u). \qquad (1.6)$$

They proved the global existence of solutions and a polynomial decay of the energy by exploiting an energy method. However the result was restricted to dimension $1 \le n \le 5$, This restriction on the space dimension was removed by Sugitani–Kawashima (see [23]) by the fundamental method of energy estimates in the Fourier (or frequency) space and some sharp decay estimates. Since the method of energy estimates in Fourier space is relatively simple and effective, it has been adapted to study some related problems (see [18, 19, 20, 24]).

For the case of dissipative plate equations of memory type, Liu–Kawashima (see [15, 12]) studied the following equation

$$u_{tt} + \Delta^2 u + u + k * \Delta u = f(u),$$

as well as the equation with rotational term

$$u_{tt}-\Delta u_{tt}+\Delta^2 u+u+k*\Delta u=f\left(u,u_t,\nabla u\right),$$

and obtained the global existence and decay estimates of solutions by the energy method in the Fourier space. The results in these papers and the general dissipative plate equation (see [13, 14, 16, 23]) show that they are of regularity-loss property.

A similar decay structure of the regularity-loss type was also observed for the dissipative Timoshenko system (see [10]) and a hyperbolic-elliptic system related to a radiating gas (see [9]). For more studies on various aspects of dissipation of plate equations, we refer to [1, 2, 3, 7]. And for the study of decay properties for hyperbolic systems of memory-type dissipation, we refer to [6, 11, 22].

The results in [12] are further studied and generalized to higher order equations in [16] and to the equations with variable coefficients in [17]. The main purpose of this paper is to study the decay estimates and regularity-loss property for solutions to the initial value problem (1.1) in the spirit of [12, 15, 16, 17]. And we generalize these results to the case of variable coefficients and semilinear equations.

The paper is arranged as follows: We study the pointwise estimates of solutions to the problem (2.2) and (2.3) in the spectral space in Section 2. And in Section 3, we prove the energy estimates and the decay estimates for solutions to the linear equation (1.3) by virtue of the estimates in Section 2. In Section 4, we prove the global existence and decay estimates for the semilinear problems (1.1).

For the reader's convenience, we give some notations which will be used below. Let $F[f]$ denote the Fourier transform of f defined by

$$F[f]=\hat{f}(\xi):=\frac{1}{(2\pi)^{\frac{n}{2}}}\int_{R^n}e^{-ix\xi}f(x)dx$$

and we denote its inverse transform as F^{-1}.

Let $L[f]$ denote the Laplace transform of f defined by

$$\|f\|_{H^s}=\left\|(1-\Delta)^{\frac{s}{2}}\ f\right\|_{L^2(R_x^n)}\cong\left\|\langle\xi\rangle^s\ \hat{f}\right\|_{L^2(R_x^n)}$$

here $\langle\xi\rangle=\left(1+|\xi|^2\right)^{\frac{1}{2}}$ denotes the Japanese bracket.

2. Pointwise estimates in the spectral space.

We observe that the equation (1.1) (respectively (1.3)) is equivalent to the following in-homeogeneous equation

$$\begin{aligned}&(1-\Delta_g)u_{tt}+(1+\Delta_g^2)u+\beta k(0)(-\Delta_g)^p u\\&\quad+\alpha u_t+\beta k'*(-\Delta_g)^p u=F(t,x)\end{aligned}\qquad(2.1)$$

with $F(t,x)=k(t)(-\Delta_g)^p u_0(x)+f(u,u_t,\nabla u)$

(respectively, $F(t,x)=k(t)(-\Delta_g)^p u_0(x)$).

In order to study the solutions to (2.1), we study the pointwise estimates for solutions to the following ODEs with parameter $\lambda\in\mathbb{R}^+$, respectively:

$$\begin{cases}(1+\lambda^2)G_{tt}(t,\lambda)+(1+\lambda^4+\beta k(0)\lambda^{2p})G(t,\lambda)\\\qquad+\alpha G_t(t,\lambda)+\beta\lambda^{2p}k'*G=0\\G(0,\lambda)=1,G_t(0,\lambda)=0,\end{cases}\qquad(2.2),$$

and

$$\begin{cases}(1+\lambda^2)H_{tt}(t,\lambda)+(1+\lambda^4+\beta k(0)\lambda^{2p})H(t,\lambda)\\\qquad+\alpha H_t(t,\lambda)+\beta\lambda^{2p}k'*H=0\\H(0,\lambda)=0,H_t(0,\lambda)=1,\end{cases}\qquad(2.3),$$

We note that $G(t,\lambda)=H_t(t,\lambda)+\langle\lambda\rangle^{-2}H(t,\lambda)$, and apply the Laplace transform to (2.2) and (2.3) (which is guaranteed by Proposition 1 given at the end of this section), then we have formally that

$$G(t,\lambda)=L^{-1}_{\tau\to t}\left[\frac{\alpha+(1+\lambda^2)\tau}{(1+\lambda^2)\tau^2+(1+\lambda^4+\beta k(0)\lambda^{2p})+\alpha\tau+\beta\lambda^{2p}L[k'](\tau)}\right](t)$$

$$H(t,\lambda)=L^{-1}_{\tau\to t}\left[\frac{(1+\lambda^2)}{(1+\lambda^2)\tau^2+(1+\lambda^4+\beta k(0)\lambda^{2p})+\alpha+\beta\lambda^{2p}L[k'](\tau)}\right](t)$$

Now by virtue of the solutions to (2.2) and (2.3), the solution to (2.1) can be expressed as

$$\begin{aligned}u(t)&=G(t,\Lambda)u_0+H(t,\Lambda)u_1\\&\quad+\int_0^t H(t-\tau,\Lambda)(1-\Delta_g)^{-1}F(\tau)d\tau\end{aligned}\qquad(2.4)$$

where $G(t,\Lambda)$ and $H(t,\Lambda)$) are defined by the measurable functional calculus (cf. [21]):

$$\begin{cases}(\varphi,\ G(t,\Lambda)\psi)=\int_R G(t,\lambda)d(P_\lambda\varphi,\psi)_{L^2}\\(\varphi,\ H(t,\Lambda)\psi)=\int_R H(t,\lambda)d(P_\lambda\varphi,\psi)_{L^2}\end{cases}\qquad(2.5)$$

for φ,ψ in the domain of $G(t,\Lambda)$ and $H(t,\Lambda)$

respectively, here $\{P_\lambda\}$ is the family of spectral projections for the positive self-adjoint operator $\Lambda=\left(-\Delta_g\right)^{\frac{1}{2}}$. We note that $G(t,\Lambda)$ and $H(t,\Lambda)$ are the solutions (formally) to the following operator equations:

$$\begin{cases}\left(1-\Delta_g\right)G_{tt}+\left(1+\Delta_g^2+\beta k(0)\left(-\Delta_g^p\right)\right)G \\ \qquad\qquad +\alpha G_t+\beta k'*\left(-\Delta_g\right)^p G=0 \qquad (2.6)\\ G(0)=I, G_t(0)=O\end{cases}$$

and

$$\begin{cases}\left(1-\Delta_g\right)H_{tt}+\left(1+\Delta_g^2+\beta k(0)\left(-\Delta_g^p\right)\right)H \\ \qquad\qquad +\alpha H_t+\beta k'*\left(-\Delta_g\right)^p H=0 \qquad (2.7)\\ H(0)=O, H_t(0)=I\end{cases}$$

respectively, here I stands for the identity operator, and O denotes the zero operator.

Thus estimates for $u(t)$ can be reduced to estimates for $G(t,\Lambda)$ and $H(t,\Lambda)$ in terms of (2.4).

First, let us introduce some notations. For any reasonable complex-valued function $f(t)$, $t\in[0,\infty)$, we define

$$(k*f)(t):=\int_0^t k(t-\tau)f(\tau)d\tau,$$
$$(k\diamond f)(t):=\int_0^t k(t-\tau)\left(f(\tau)-f(t)\right)d\tau,$$
$$(k\square f)(t):=\int_0^t k(t-\tau)\left|f(t)-f(\tau)\right|^2 d\tau.$$

Then direct computations imply the following lemma

Lemma 2.1. For any functions $k\in C^1(R^+)$ and $\phi\in H^1(R^+)$, it holds that

$$(1).\quad (k*\phi)(t)=(k\diamond\phi)(t)+\left(\int_0^t k(\tau)d\tau\right)\phi(t),$$

$$(2).\quad \mathrm{Re}\left\{(k*\phi)(t)\bar{\phi}_t(t)\right\}=-\frac{1}{2}k(t)|\phi(t)|^2$$
$$+\frac{1}{2}(k'\square\phi)(t)-\frac{1}{2}\frac{d}{dt}\left\{(k\square\phi)(t)-\left(\int_0^t k(\tau)d\tau\right)|\phi(t)|^2\right\}$$

$$(3).\quad \left|(k\diamond\phi)(t)\right|^2\le\left(\int_0^t|k(\tau)|d\tau\right)(|k|\square\phi)(t).$$

Remark 2. From Lemma 2.1 1), we have

$$(k*\phi)_t=k(0)\phi+k'*\phi=k(t)\phi+k'\diamond\phi.$$

Now we come to get the pointwise estimates of $G(t,\lambda)$ and $H(t,\lambda)$ in the spectral space, and we have the following proposition.

Proposition 1 (pointwise estimates in the spectral space). Assume $G(t,\lambda)$ and $H(t,\lambda)$ are the solutions of (2.2) and (2.3) respectively, then they satisfy the following estimates:

$$\left|\langle\lambda\rangle G_t(t,\lambda)\right|^2+\left|\langle\lambda\rangle^2 G(t,\lambda)\right|^2$$
$$+\beta|\lambda|^{2p}(k\square G)(t,\lambda)\le Ce^{-c\rho(\lambda)t}\langle\lambda\rangle^4,$$

And

$$\left|\langle\lambda\rangle H_t(t,\lambda)\right|^2+\left|\langle\lambda\rangle^2 H(t,\lambda)\right|^2$$
$$+\beta|\lambda|^{2p}(k\square H)(t,\lambda)\le Ce^{-c\rho(\lambda)t}\langle\lambda\rangle^4,$$

here $k\square G$ and $k\square H$ are defined as in (2.8), and

$$\rho(\lambda)=\langle\lambda\rangle^{-2}\text{ with }\langle\lambda\rangle=\left(1+\lambda^2\right)^{\frac{1}{2}}.$$

Proof. We only prove the estimate for $G(t,\lambda)$, and the case for $H(t,\lambda)$ can be proved in a similar way. To simplify the notation in the following, we write G for $G(t,\lambda)$.

Step 1. By multiplying (2.2) by $\bar{G}_t$ and taking the real part, we have that

$$\left\{\frac{1}{2}\langle\lambda\rangle^2|G_t|^2\right\}_t+\left\{\frac{1}{2}\left(1+\lambda^4+\beta\lambda^{2p}k(t)\right)|G|^2\right\}$$
$$+\alpha|G_t|^2+\beta\lambda^{2p}\,\mathrm{Re}\left\{(k'*G)\bar{G}_t\right\}=0 \qquad (2.9)$$

Apply Lemma 2.1 2) to the term $\mathrm{Re}\left\{(k'*G)\bar{G}_t\right\}$ in (2.9), and denote

$$E_1(t,\lambda):=\frac{1}{2}\left(1+\lambda^2\right)|G_t|^2+\frac{1}{2}\left(1+\lambda^4+\beta\lambda^{2p}k(t)|G|^2\right)$$
$$-\frac{\beta\lambda^{2p}}{2}(k'\square G),$$

and

$$\left|R_2(t,\lambda)\right| \le C\left(\langle\lambda\rangle^2 |G_t|^2 + \frac{\beta\lambda^{2p}}{2}k(0)|G|^2\right) + \frac{\beta\lambda^{2p}}{2}(k''\Box G),$$

then we obtain that

$$\frac{\partial}{\partial t}E_1(t,\lambda) + F_1(t,\lambda) = 0. \qquad (2.10)$$

Step 2. By multiplying (2.2) by $\bar{G}$ and taking the real part, we have that

$$\begin{aligned}&\mathrm{Re}\left\{\left(1+\lambda^2\right)G_t\bar{G}\right\}_t - \left(1+\lambda^2\right)|G_t|^2 \\ &\quad + \left(1+\lambda^4+\beta k(0)\lambda^{2p}\right)|G|^2 + \alpha\left\{\frac{1}{2}|G|^2\right\}_t \\ &\quad + \beta\lambda^{2p}\,\mathrm{Re}\left\{(k'*G)\bar{G}\right\} = 0. \qquad (2.11)\end{aligned}$$

In view of Lemma 2.1 1), we have that

$$\begin{aligned}\mathrm{Re}\left\{(k'*G)\bar{G}\right\} &= \mathrm{Re}\left\{(k'\Diamond G)\bar{G}\right\} + \left(\int_0^t k'(\tau)d\tau\right)G\bar{G} \\ &= \mathrm{Re}\left\{(k'\Diamond G)\bar{G}\right\} + \left(k(t)-k(0)\right)|G|^2\end{aligned}$$

Denote

$$\begin{aligned}E_2(t,\lambda) &:= \mathrm{Re}\left\{\left(1+\lambda^2\right)G_t\bar{G}\right\} + \frac{\alpha}{2}|G|^2, \\ F_2(t,\lambda) &:= \left(1+\lambda^4+\beta k(t)\lambda^{2p}\right)|G|^2, \\ R_2(t,\lambda) &:= \left(1+\lambda^2\right)|G_t|^2 - \beta\lambda^{2p}\,\mathrm{Re}\left\{(k'\Diamond G)\bar{G}\right\},\end{aligned}$$

then (2.11) yields that

$$\frac{\partial}{\partial t}E_2(t,\lambda) + F_2(t,\lambda) = R_2(t,\lambda). \qquad (2.12)$$

Step 3. Define $\rho(\lambda) = \langle\lambda\rangle^{-2}$, and set

$$\begin{aligned}E(t,\lambda) &:= E_1(t,\lambda) + \gamma\rho(\lambda)E_2(t,\lambda), \\ F(t,\lambda) &:= F_1(t,\lambda) + \gamma\rho(\lambda)F_2(t,\lambda), \\ R(t,\lambda) &:= \gamma\rho(\lambda)R_2(t,\lambda),\end{aligned}$$

Here γ is a positive constant and will be determined later. Then (2.10) and (2.12) yields that

$$\frac{\partial}{\partial t}E(t,\lambda) + F(t,\lambda) = R(t,\lambda). \qquad (2.13)$$

We introduce the following Lyapunov functions:

$$\begin{aligned}E_0(t,\lambda) &:= \frac{1}{2}\left(1+\lambda^2\right)|G_t|^2 + \frac{1}{2}\left(1+\lambda^4\right)|G|^2 + \frac{1}{2}\beta\lambda^{2p}(k\Box G), \\ F_0(t,\lambda) &:= |G_t|^2 + \frac{\beta\lambda^{2p}}{2}k(t)|G|^2 + \frac{\beta\lambda^{2p}}{2}(k''\Box G).\end{aligned}$$

From the definition of $E_1(t,\lambda)$ and $F_1(t,\lambda)$, we know that there exist positive constants $C_i\ (i=1,2,3)$ such that the following estimates hold:

$$\begin{aligned}&C_1E_0(t,\lambda) \le E_1(t,\lambda) \le C_2E_0(t,\lambda), \\ &F_1(t,\lambda) \ge C_3F_0(t,\lambda). \qquad (2.14)\end{aligned}$$

On the other hand, since

$$\left|E_2(t,\lambda)\right| \le C\left(\langle\lambda\rangle^4|G_t|^2 + |G|^2\right),$$

we know that

$$\begin{aligned}\gamma\rho(\lambda)\left|E_2(t,\lambda)\right| &\le \gamma C\left(\langle\lambda\rangle^2|G_t|^2 + \left(1+\lambda^4\right)|G|^2\right) \\ &\quad + \gamma C\left(\frac{\beta\lambda^{2p}}{2}(k\Box G)\right) \le \gamma C_4E_0(t,\lambda).\end{aligned}$$

Choosing γ suitably small such that $\gamma C_4 \le \min\left\{\frac{C_1}{2}, \frac{C_2}{2}\right\}$, and by virtue of (2.14), we have that

$$\frac{C_1}{2}E_0(t,\lambda) \le E(t,\lambda) \le \frac{3C_2}{2}E_0(t,\lambda). \qquad (2.15)$$

In view of (2.14), it is easy to verify that

$$F(t,\lambda) \ge C_3F_0(t,\lambda) + C_3\gamma\rho(\lambda)\left(1+\lambda^4+\beta k(t)\lambda^{2p}\right)|G|^2 \qquad (2.16)$$

Since

$$\begin{aligned}\left|R_2(t,\lambda)\right| &\le C\left(\langle\lambda\rangle^2|G_t|^2 + \frac{\beta\lambda^{2p}}{2}k(0)|G|^2\right) \\ &\quad + C\frac{\beta\lambda^{2p}}{2}(k''\Box G).\end{aligned}$$

We have

$$\begin{aligned}\left|R(t,\lambda)\right| &\le \gamma C\left(|G_t|^2 + \rho\langle\lambda\rangle\frac{\beta\lambda^{2p}}{2}k(0)|G|^2\right) \\ &\quad + \gamma C\rho(\lambda)\frac{\beta\lambda^{2p}}{2}(k''\Box G) \\ &\le \gamma C_5F(t,\lambda).\end{aligned}$$

Taking γ sufficiently small such that

$\gamma \le \left\{ \frac{1}{2C_5}, C_4^{-1} \min\left\{ \frac{C_1}{2}, \frac{C_2}{2} \right\} \right\}$, we have that

$$\left| R(t,\lambda) \right| \le \frac{1}{2} F(t,\lambda). \qquad (2.17)$$

In view of (2.13), the relation (2.17) yields that

$$\frac{\partial}{\partial t} E(t,\lambda) + \frac{1}{2} F(t,\lambda) \le 0. \qquad (2.18)$$

On the other hand, (2.15) and (2.16) yield that

$$F(t,\lambda) \ge c\rho(\lambda) E(t,\lambda) \qquad (2.19)$$

Then (2.18) and (2.19) yield that

$$E(t,\lambda) \le e^{-c\rho(\lambda)} E(0,\lambda) \qquad (2.20)$$

By virtue of (2.15) and (2.20), we get the desired results.

3. Decay estimates of solutions to the linear problem.

In this section we shall use the functional calculus of Λ and the pointwise estimates in spectral space obtained in Proposition 1 to prove the energy estimate in Theorem 1.1 and the decay estimates in Theorem 1.2.

Proof of Theorem 1.1. From (2.18) and (2.19) we have that

$$\frac{\partial}{\partial t} E(t,\lambda) + C\rho(\lambda) E(t,\lambda) \le 0.$$

Integrate the previous inequality with respect to t and appeal to (2.15), then we obtain

$$E_0(t,\lambda) + \int_0^t \rho(\lambda) E_0(\tau,\lambda) \le C E_0(t,\lambda). \qquad (3.1)$$

Multiply (3.1) by $\langle \lambda \rangle^{2(s-1)}$ and integrate the resulting inequality with respect to the measure $d\left(P_\lambda u_0, u_0\right)$, as well as by the definition of $G(t,\Lambda)$ in (2.5) and the equivalence (1.2), then we obtain the following estimate for $G(t,\Lambda)u_0$:

$$\begin{aligned} &\left\| G(t,\Lambda)u_0 \right\|_{H^{s+1}}^2 + \left\| G_t(t,\Lambda)u_0 \right\|_{H^s}^2 \\ &\quad + \int_0^t \left(\left\| G(\tau,\Lambda)u_0 \right\|_{H^s}^2 + \left\| G_t(\tau,\Lambda)u_0 \right\|_{H^{s-1}}^2 \right) d\tau \\ &\quad \le C \left\| u_0 \right\|_{H^{s+1}}^2. \end{aligned} \qquad (3.2)$$

Similarly, we have

$$\begin{aligned} &\left\| H(t,\Lambda)u_1 \right\|_{H^{s+1}}^2 + \left\| H_t(t,\Lambda)u_1 \right\|_{H^s}^2 \\ &\quad + \int_0^t \left(\left\| H(\tau,\Lambda)u_1 \right\|_{H^s}^2 + \left\| H_t(\tau,\Lambda)u_1 \right\|_{H^{s-1}}^2 \right) d\tau \\ &\quad \le C \left\| u_1 \right\|_{H^{s+1}}^2. \end{aligned} \qquad (3.3)$$

From (3.3), we know that

$$\left\| H(t,\Lambda)u_1 \right\|_{H^{s+1}} \le C \left\| u_1 \right\|_{H^s}, \quad \forall u_1 \in S(\mathbb{R}^n), t > 0, \qquad (3.4)$$

which implies

$$\begin{aligned} &\left\| \int_0^t k(\tau) H(\tau,\Lambda) \left(-\Delta_g\right)^p \left(1-\Delta_g\right)^{-1} u_0 d\tau \right\|_{H^{s+1}} \\ &\le \int_0^t k(\tau) d\tau \sup_{\tau \in [0,t]} \left\| H(\tau,\Lambda) \left(-\Delta_g\right)^p \left(1-\Delta_g\right)^{-1} u_0 \right\|_{H^{s+1}} \\ &\le C \left\| u_0 \right\|_{H^{s+2p-2}}. \end{aligned} \qquad (3.5)$$

Similarly, we have

$$\begin{aligned} &\left\| \int_0^t k(\tau) H_t(\tau,\Lambda) \left(-\Delta_g\right)^p \left(1-\Delta_g\right)^{-1} u_0 d\tau \right\|_{H^s} \\ &\le \int_0^t k(\tau) d\tau \sup_{\tau \in [0,t]} \left\| H_t(\tau,\Lambda) \left(-\Delta_g\right)^p \left(1-\Delta_g\right)^{-1} u_0 \right\|_{H^s} \\ &\le C \left\| u_0 \right\|_{H^{s+2p-2}}. \end{aligned} \qquad (3.6)$$

Again from (3.3), we know that

$$\left\| H_t(t,\Lambda)u_1 \right\|_{H^s}^2 \le C \left\| u_1 \right\|_{H^s}^2, \quad \forall u_1 \in S(\mathbb{R}^n), t > 0.$$

which implies that

$$\begin{aligned} &\int_0^t \left\| \int_0^\tau k(\sigma) H(\tau-\sigma,\Lambda) \left(-\Delta_g\right)^p \left(1-\Delta_g\right)^{-1} u_0 d\sigma \right\|_{H^s}^2 d\tau \\ &\le \left\| k \right\|_{L^1} \left(\int_0^t k(\sigma) \left\| H(\tau-\sigma,\Lambda) \left(-\Delta_g\right)^p \left(1-\Delta_g\right)^{-1} u_0 \right\|_{H^s}^2 d\sigma \right) d\tau \\ &\le \left\| k \right\|_{L^1}^2 \int_0^t \left\| H(\tau-\sigma,\Lambda) \left(-\Delta_g\right)^p \left(1-\Delta_g\right)^{-1} u_0 \right\|_{H^s}^2 d\tau \\ &\le C \left\| u_0 \right\|_{H^{s+2p-2}}^2 \end{aligned} \qquad (3.7)$$

where in the first inequality, we used the Jensen's inequality, while in the second inequality, we used the L^1-estimates for the convolution operation with respect to time (or changing the order of integration).

In a similar way, by (3.3), we have

$$\int_0^t \left\| \int_0^\tau k(\sigma) H_t(\tau-\sigma,\Lambda)\left(-\Delta_g\right)^p \left(1-\Delta_g\right)^{-1} u_0 d\sigma \right\|_{H^{s-1}}^2 d\tau$$
$$\le \|k\|_{L^1} \left(\int_0^t k(\sigma) \left\| H_t(\tau-\sigma,\Lambda)\left(-\Delta_g\right)^p \left(1-\Delta_g\right)^{-1} u_0 \right\|_{H^{s-1}}^2 d\sigma \right) d\tau$$
$$\le \|k\|_{L^1}^2 \int_0^t \left\| H_t(\tau-\sigma,\Lambda)\left(-\Delta_g\right)^p \left(1-\Delta_g\right)^{-1} u_0 \right\|_{H^{s-1}}^2 d\tau$$
$$\le C \|u_0\|_{H^{s+2p-2}}^2 \qquad (3.8)$$

Thus, in term of (2.4) and the estimates of (3.2)–(3.8), as well as the fact that

$$u_t(t) = G_t(t,\Lambda)u_0 + H_t(t,\Lambda)u_1 + \int_0^t H_t(t-\tau,\Lambda)\left(1-\Delta_g\right)^{-1} F(\tau)\, d\tau. \qquad (3.9)$$

with $F(t,x) = k(t)\left(-\Delta_g\right)^p u_0(x)$ defined in (2.1), we have

$$\|u(t)\|_{H^{s+1}}^2 + \|u_t(t)\|_{H^s}^2 + \int_0^t \left(\|u(\tau)\|_{H^s}^2 + \|u_t(\tau)\|_{H^{s-1}}^2 \right) d\tau \le C I_0^2.$$

That is the conclusion of the theorem.

In order to prove Theorem 1.2, we need the following lemma which is a direct result of Proposition 1.

Lemma 3.1. With $\rho(\lambda) = \langle\lambda\rangle^{-2}$ introduced in Proposition 1, $G(t,\lambda)$ and $H(t,\lambda)$ satisfy the following estimates:

$$(1).\left|G(t,\lambda)\right| \le Ce^{-c\rho(\lambda)t}$$
$$(2).\left|G_t(t,\lambda)\right| \le Ce^{-c\rho(\lambda)t}\langle\lambda\rangle,$$
$$(3).\left|H(t,\lambda)\right| \le Ce^{-c\rho(\lambda)t}\langle\lambda\rangle^{-1},$$
$$(1).\left|H_t(t,\lambda)\right| \le Ce^{-c\rho(\lambda)t}.$$

By the above lemma, we have the following estimates:

Lemma 3.2. Let $r \ge 0, \upsilon \ge 0$ be real numbers, then the following estimates hold:

$$(1).\left\|G(t,\Lambda)\varphi\right\|_{H^r} \le C(1+t)^{-\frac{\upsilon}{2}} \|\varphi\|_{H^{r+\upsilon}}, \forall \varphi \in S(\mathbb{R}^n),$$
$$(2).\left\|G_t(t,\Lambda)\varphi\right\|_{H^r} \le C(1+t)^{-\frac{\upsilon}{2}} \|\varphi\|_{H^{r+\upsilon+1}}, \forall \varphi \in S(\mathbb{R}^n),$$
$$(3).\left\|H(t,\Lambda)\varphi\right\|_{H^r} \le C(1+t)^{-\frac{\upsilon}{2}} \|\varphi\|_{H^{r+\upsilon-1}}, \forall \varphi \in S(\mathbb{R}^n),$$
$$(4).\left\|H_t(t,\Lambda)\varphi\right\|_{H^r} \le C(1+t)^{-\frac{\upsilon}{2}} \|\varphi\|_{H^{r+\upsilon}}, \forall \varphi \in S(\mathbb{R}^n).$$

Proof. We only prove the case 1), but the other cases can be deduced similarly. In view of Lemma 3.1 1) and the functional calculus (2.5) as well as the equivalence (1.2), we have that

$$\begin{aligned}\left\|G(t,\Lambda)\phi\right\|_{H^r}^2 &\le C\int_0^\infty \langle\lambda\rangle^{2r} \left|G(t,\lambda)\right| d(P_\lambda\phi,\phi)_{L^2} \\ &\le C\int_0^\infty \langle\lambda\rangle^{2r} e^{-cp(\lambda)t} d(P_\lambda\phi,\phi)_{L^2} \\ &= C\int_0^1 \langle\lambda\rangle^{2r} e^{-cp(\lambda)t} d(P_\lambda\phi,\phi)_{L^2} \\ &\quad + C\int_0^\infty \langle\lambda\rangle^{2r} e^{-cp(\lambda)t} d(P_\lambda\phi,\phi)_{L^2} \\ &=: I_1 + I_2.\end{aligned}$$

It is obvious that

$$I_1 \le Ce^{-ct}\left\|\phi\right\|_{L^2}^2.$$

On the other hand,

$$I_2 \le C(1+t)^{-\nu}\int_0^\infty \langle\lambda\rangle^{2(r+\nu)} d(P_\lambda\varphi,\varphi)_{L^2} \le C(1+t)^{-\nu}\left\|\varphi\right\|_{H^{r+\nu}}^2.$$

Here

$$r \ge 0, \nu \ge 0, r+\nu \le s + \max\{1, 2p-2\}.$$

Thus the result for the case 1) is proved.

Proof of Theorem 1.2. Let $r \ge 0$, then from (2.4) we have that

$$\begin{aligned}\left\|u(t)\right\|_{H^r} &\le \left\|G(t,\Lambda)u_0\right\|_{H^r} + \left\|H(t,\Lambda)u_1\right\|_{H^r} \\ &\quad + \left\| \int_0^t k(\tau) H(t-\tau,\Lambda)(-\Delta_g)^p (1-\Delta_g)^{-1} u_0 d_\tau \right\|_{H^r} \\ &= I + II + III.\end{aligned}$$

By Lemma 3.2, we know that

$$I + II \le C(1+t)^{-\frac{\nu_1}{2}} \left\|u_0\right\|_{H^{r+\nu_1}} + C(1+t)^{-\frac{\nu_2}{2}} \left\|u_1\right\|_{H^{r+\nu_2-1}}.$$

And

$$III \le \int_0^{\frac{t}{2}} k(\tau) \left\| H(t-\tau,\Lambda)(-\Delta_g)^p (1-\Delta_g)^{-1} u_0 \right\|_{H^r} d\tau + \int_{\frac{t}{2}}^t k(\tau) \left\| H(t-\tau,\Lambda)(-\Delta_g)^p (1-\Delta_g)^{-1} u_0 \right\|_{H^r} d\tau$$
$$\le C(1+t)^{-\frac{\nu_3}{2}} \left\| (-\Delta_g)^p (1-\Delta_g)^{-1} u_0 \right\|_{H^{r+\nu_3-1}} \int_0^{\frac{t}{2}} k(\tau) d\tau + Ce^{-ct} \left\| (-\Delta_g)^p (1-\Delta_g)^{-1} u_0 \right\|_{H^{r+\nu_3-1}}$$
$$\le C(1+t)^{-\frac{\nu_3}{2}} \left\|u_0\right\|_{H^{r+\nu_3+2p-3}},$$

where in the second step, we used the exponentially decay

property of $k(t)$, which is a direct result from the Assumption [A]. Thus, we have

$$\begin{aligned}\|u(t)\|_{H^r} &\le C(1+t)^{-\frac{v_1}{2}}\|u_0\|_{H^{r+(v_1-\max\{1,2p-2\}+1)-1+\max\{1,2p-2\}}}\\ &+C(1+t)^{-\frac{v_2}{2}}\|u_1\|_{H^{r+v_2-1}}\\ &+(1+t)^{-\frac{v_3}{2}}\|u_0\|_{H^{r+(v_3+2p-2-\max\{1,2p-2\}+1)-1+\max\{1,2p-2\}}}.\end{aligned}$$

Here $v_1 \ge 0, v_2 \ge 0, v_3 \ge 0$ satisfy

$$\begin{cases} r+v_1 \le s+\max\{1,2p-2\},\\ r+v_2-1 \le s,\\ r+v_3+2p-3 \le s+\max\{1,2p-2\}. \end{cases} \quad (3.10)$$

Choose the smallest real numbers v_1, v_2, v_3 such that

$$\begin{cases} v_1-\max\{1,2p-2\}+1 \ge \sigma,\\ v_2 \ge \sigma,\\ v_3+2p-2-\max\{1,2p-2\} \ge \sigma. \end{cases}$$

It gives that

$$\begin{cases} v_2=\sigma,\\ v_1=v_2+\max\{1,2p-2\}-1,\\ v_3=v_2+\max\{1,2p-2\}-(2p-2). \end{cases}$$

Thus, the inequality (3.10) holds with r satisfying

$$0 \le r \le s+1-\sigma.$$

Taking the maximal r , i.e., $r=s+1-\sigma$, we obtain

$$\|u(t)\|_{H^{s+1-\sigma}} \le CI_0(1+t)^{-\frac{\sigma}{2}}.$$

That is the result for $u(t)$.

The estimate for $u_t(t)$ can be proved in a similar way by just using the fact (3.9) and Lemma 3.2, and we omit the details.

4. Global existence and decay estimates of solutions to the semilinear problem.

In this section, by virtue of the properties of solution operators, we prove the global existence and optimal decay estimates of solutions to the semilinear problem by employing the contraction mapping theorem.

From (2.1), we know that the solution to (1.1) can be expressed as

$$\begin{aligned}u(t) &= G(t,\Lambda)u_0+H(t,\Lambda)u_1\\ &+\int_0^t H(t-\tau,\Lambda)k(\tau)(1-\Delta_g)^{-1}(-\Delta_g)^p u_0 d\tau\\ &+\int_0^t H(t-\tau,\Lambda)(1-\Delta_g)^{-1} f(u(\tau),u_t(\tau),\nabla u(\tau))d\tau.\end{aligned}$$

Lemma 4.1 (Moser estimates). Assume that $r \ge 0$ be a real number, then

$$\|uv\|_{H^r} \le C(\|u\|_{L^\infty}\|v\|_{H^r}+\|v\|_{L^\infty}\|u\|_{H^r}).$$

By the previous lemma and an inductive argument, we have the following estimates:

Lemma 4.2. Assume that $\alpha \ge 1, \beta \ge 1$ be integers, and $r \ge 0$ be a real number, then

$$\begin{aligned}\|u^\alpha v^\beta\|_{H^r} \le C(&\|u\|_{L^\infty}^{\alpha-1}\|v\|_{L^\infty}^{\beta-1}(\|u\|_{L^\infty}\|v\|_{H^r}\\ &+\|v\|_{L^\infty}\|u\|_{H^r}).\end{aligned}$$

Define

$$\begin{aligned}X := \{&u \in C([0,\infty),H^{s+1}(\mathbb{R}^n)) \cap\\ &C^1([0,\infty),H^s(\mathbb{R}^n));\|u\|<+\infty\},\end{aligned}$$

here

$$\begin{aligned}\|u\|_X := &\sup_{0\le\sigma\le s+1}\sup_{t\ge0}\{(1+t)^{\frac{\sigma}{2}}\|u(t)\|_{H^{s+1-\sigma}}\}\\ &+\sup_{0\le\sigma\le s+1}\sup_{t\ge0}\{(1+t)^{\frac{\sigma}{2}}\|u_t(t)\|_{H^{s-\sigma}}\}.\end{aligned}$$

Proposition 2. There exists $C>0$ such that

$$\|U(t)\|_{L^\infty} \le C\|u\|_X. \quad (4.1)$$

Proof. By the Sobolev imbedding theorems, we have

$$\|U(t)\|_{L^\infty} \le C\|U(t)\|_{H^s}.$$

By the definition of $\|u\|_X$ and $\|\nabla u\|_{H^s} \le C\|u\|_{H^{s+1}}$, we obtained the result.

Denote

$$\begin{aligned}&B_R := \{u \in X; \|u\|_X \le R\},\\ &U := (u,u_t,\nabla u),\\ &\Phi[u](t) := \Phi_0(t)+\int_0^t H(t-\tau,\Lambda)(1-\Delta_g)^{-1} f(U)d\tau,\\ &\Phi_0(t) := G(t,\Lambda)u_0+H(t,\Lambda)u_1\\ &+\int_0^t H(t-\tau,\Lambda)k(\tau)(1-\Delta_g)^{-1}(-\Delta_g)^p u_0 d\tau.\end{aligned}$$

We will prove that $u \to \Phi(u)$ is a contraction mapping on B_R for some $R>0$.

Proof of Theorem 1.3. We denote

$V := (v, v_t, \nabla v)$, $W := (w, w_t, \nabla w)$,then

$$\Phi[v](t) - \Phi[w](t) = \int_0^t H(t-\tau, \Lambda)(1-\Delta_g)^{-1}(f(V) - f(W))(\tau)d\tau.$$

Step 1: We prove:

$$\left\|\Phi[v](t) - \Phi[w](t)\right\|_{H^{s+1-\sigma}} \le C(1+t)^{-\frac{\sigma}{2}} \left\|(v,w)\right\|_X^{\eta-1} \left\|v-w\right\|_X \qquad (4.2)$$

and $0 \le \sigma \le s+1$

Indeed,

$$\left\|(\Phi[v]-\Phi[w])(t)\right\|_{H^{s+1-\sigma}} \le \left(\int_0^{\frac{t}{2}} + \int_{\frac{t}{2}}^t\right) \left\|H(t-\tau,\Lambda)(1-\Delta_g)^{-1}(f(V)-f(W))(\tau)\right\|_{H^{s+1-\sigma}} d\tau$$

$$\le \left(\int_0^{\frac{t}{2}} + \int_{\frac{t}{2}}^t\right) \left\|H(t-\tau,\Lambda)(1-\Delta_g)^{-1}(f(V)-f(W))(\tau)\right\|_{H^{s+1-\sigma-2}} d\tau =: I_1 + I_2. \qquad (4.3)$$

In view of lemma 3.2 3), we have that

$$I_1 \le C\int_0^{\frac{t}{2}} (1+t-\tau)^{-\frac{v}{2}} \left\|(f(V)-f(W))(\tau)\right\|_{H^{s+1-\sigma-2+v-1}} d\tau \le C\int_0^{\frac{t}{2}} (1+t-\tau)^{-\frac{v}{2}} \left\|(f(V)-f(W))(\tau)\right\|_{H^{s+1-(\sigma-v-3)}} d\tau \qquad (4.4)$$

By Lemma 4.2, we get that

$$\left\|(f(V)-f(W))(\tau)\right\|_{H^{s+1-[\sigma-(v-3)]}} \le C\left\|(V,W)(\tau)\right\|_{L^\infty}^{\eta-2} \times\{\left\|(V,W)(\tau)\right\|_{L^\infty} \left\|(V-W)(\tau)\right\|_{H^{s+1-[\sigma-(v-3)]}} + \left\|(V+W)(\tau)\right\|_{H^{s+1-[\sigma-(v-3)]}} \left\|(V-W)(\tau)\right\|_{L^\infty}\}.$$

In view of (4.1), we have that

$$\left\|(f(V)-f(W))(\tau)\right\|_{H^{s+1-[\sigma-(v-3)]}} \le C(1+\tau)^{-\frac{\sigma-(v-3)}{2}} \left\|(v,w)\right\|_X^{\eta-1} \left\|(v,w)\right\|_X d\tau \qquad (4.5)$$

Let $v = \sigma$ in (4.5), we have that

$$I_1 \le C\int_0^{\frac{t}{2}} (1+t-\tau)^{-\frac{v}{2}} (1+\tau)^{-\frac{\sigma-(v-3)}{2}} \left\|(v,w)\right\|_X^{\eta-1} \left\|(v-w)\right\|_X d\tau \le C\int_{\frac{t}{2}}^t (1+\frac{t}{2})^{-\frac{\sigma}{2}} \int_0^{\frac{t}{2}} (1+\tau)^{-\frac{-3}{2}} \left\|(v,w)\right\|_X^{\eta-1} \left\|(v-w)\right\|_X d\tau \le C(1+t)^{-\frac{\sigma}{2}} \left\|(v,w)\right\|_X^{\eta-1} \left\|(v-w)\right\|_X . \qquad (4.6)$$

Le $v = 0$ in (4.5), we have that

$$I_2 \le C\int_{\frac{t}{2}}^t (1+t-\tau)^{-\frac{v}{2}} (1+\tau)^{-\frac{\sigma-(v-3)}{2}} \left\|(v,w)\right\|_X^{\eta-1} \left\|(v-w)\right\|_X d\tau \le C\int_{\frac{t}{2}}^t (1+t)^{-\frac{\sigma+3}{2}} \left\|(v,w)\right\|_X^{\eta-1} \left\|(v-w)\right\|_X d\tau \le C\int_{\frac{t}{2}}^t (1+\frac{t}{2})^{-\frac{\sigma}{2}} (1+\tau)^{-\frac{3}{2}} \left\|(v,w)\right\|_X^{\eta-1} \left\|(v-w)\right\|_X d\tau \le C(1+t)^{-\frac{\sigma}{2}} \left\|(v,w)\right\|_X^{\eta-1} \left\|(v-w)\right\|_X . \qquad (4.7)$$

By virtue of (4.6) and (4.7), we obtain the desired results.

Step 2. we prove:

$$\left\|(\Phi_t[v]-\Phi_t[w])(t)\right\|_{H^{s-\sigma}} \le C(1+t)^{-\frac{\sigma}{2}} \left\|(v,w)\right\|_X^{\eta-1} \left\|(v-w)\right\|_X . \qquad (4.8)$$

Indeed,

$$\left\|(\Phi_t[v]-\Phi_t[w])(t)\right\|_{H^{s-\sigma}} \le \left(\int_0^{\frac{t}{2}} + \int_{\frac{t}{2}}^t\right) \left\|H_t(t-\tau,\Lambda)(1-\Delta_g)^{-1}(f(V)-f(W))(\tau)\right\|_{H^{s-\sigma}} d\tau \le \left(\int_0^{\frac{t}{2}} + \int_{\frac{t}{2}}^t\right) \left\|H_t(t-\tau,\Lambda)(f(V)-f(W))(\tau)\right\|_{H^{s-\sigma-2}} d\tau =: I_3 + I_4.$$

In view of Lemma 3.2 4), we have

$$I_3 \le C\int_0^{\frac{t}{2}} (1+t-\tau)^{-\frac{v}{2}} \left\|(f(V)-f(W))(\tau)\right\|_{H^{s+v-\sigma-2}} d\tau = C\int_0^{\frac{t}{2}} (1+t-\tau)^{-\frac{v}{2}} \left\|(f(V)-f(W))(\tau)\right\|_{H^{s+1-[\sigma-(v-3)]}} d\tau.$$

In a similar way to (4.6) and (4.7), we have

$$I_3 \le$$

$$C\int_0^{\frac{t}{2}}(1+t-\tau)^{-\frac{\nu}{2}}(1+\tau)^{-\frac{\sigma-(\nu-3)}{2}}\|(v,w)\|_X^{\eta-1}\|(v-w)\|_X d\tau$$

$$\le C\int_{\frac{t}{2}}^{t}(1+\frac{t}{2})^{-\frac{\sigma}{2}}\int_0^{\frac{t}{2}}(1+\tau)^{-\frac{-3}{2}}\|(v,w)\|_X^{\eta-1}\|(v-w)\|_X d\tau$$

$$\le C(1+t)^{-\frac{\sigma}{2}}\|(v,w)\|_X^{\eta-1}\|(v-w)\|_X . \qquad (4.9)$$

and

$$I_4 \le$$

$$C\int_{\frac{t}{2}}^{t}(1+t-\tau)^{-\frac{\nu}{2}}(1+\tau)^{-\frac{\sigma-(\nu-3)}{2}}\|(v,w)\|_X^{\eta-1}\|(v-w)\|_X d\tau$$

$$\le C\int_{\frac{t}{2}}^{t}(1+t)^{-\frac{\sigma+3}{2}}\|(v,w)\|_X^{\eta-1}\|(v-w)\|_X d\tau$$

$$\le C\int_{\frac{t}{2}}^{t}(1+\frac{t}{2})^{-\frac{\sigma}{2}}(1+\tau)^{-\frac{3}{2}}\|(v,w)\|_X^{\eta-1}\|(v-w)\|_X d\tau$$

$$\le C(1+t)^{-\frac{\sigma}{2}}\|(v,w)\|_X^{\eta-1}\|(v-w)\|_X . \qquad (4.10)$$

By virtue of (4.9) and (4.10), we obtain the desired results.

Combining the estimates (4.2) and (4.8), we obtain that

$$\|\Phi[v]-\Phi[w]\|_X \le C\|(v,w)\|_X^{\eta-1}\|v-w\|_X . \qquad (4.11)$$

So far we proved that

$$\|\Phi[v]-\Phi[w]\|_X \le C_1 R^{\eta-1}\|v-w\|_X \text{ if } v,w \in B_R .$$

On the other hand, $\Phi(0)(t)=\Phi_0(t)$, and from Theorem 1.2 we know that $\|\Phi[0]\|_X \le C_2 I_0$ if I_0 is suitably small.Take $R=2C_2I_0$. if I_0 is suitably small such that

$C_1R^{\eta-1} \le \frac{1}{2}$, then we have that

$$\|\Phi[v]-\Phi[w]\|_X \le \frac{1}{2}\|v-w\|_X .$$

It yields that, for $v \in B_R$,

$$\|\Phi[v]\|_X \le \|\Phi[0]\|_X + \frac{1}{2}\|v\|_X \le C_2I_0 + \frac{1}{2}R = R$$

Thus $\Phi[v] \in B_R$, $v \to \Phi[v]$ is a contraction mapping on B_R .and by the fixed point theorem there exists a unique $u \in B_R$ satisfying $\Phi[u]=u$,

and it is the solution to the semilinear problem (1.1) satisfying the decay estimates (1.4) and (1.5). So far we complete the proof of Theorem 1.3.

4. REFERENCES

[1] M. E. Bradley and S. Lenhart, Bilinear spatial control of the velocity term in a Kirchhoff plate equation, Electronic J. Differential Equations, 2001 (2001), 1-15.

[2] C. Buriol, Energy decay rates for the Timoshenko system of thermoelastic plates,Nonlinear Analysis, 64 (2006), 92-108.

[3] R. C. Charão, E. Bisognin, V. Bisognin and A.F. Pazoto, Asymptotic behavior for a dissipative plate equation in R N with periodic coefficients, Electronic J. Differential Equations, 2008 (2008), 1-23.

[4] C. R. da Luz and R. C. Charão, Asymptotic properties for a semi-linear plate equation in unbounded domains, J. Hyperbolic Differential Equations, 6 (2009), 269-294.

[5] M. Dimassi and J. Sjöstrand, Spectral Asymptotics in the Semi-Classical Limit, London Mathematical Society Lecture Note Series, 268, Cambridge University Press, (1999).

[6] P. M. N. Dharmawardane, J. E. Muñoz Rivera and S. Kawashima, Decay property for second order hyperbolic systems of viscoelastic materials, J. Math. Anal. Appl., 366(2010), 621-635.

[7] Y. Enomoto, On a thermoelastic plate equation in an exterior domain, Math. Meth.Appl. Sci., 25 (2002), 443-472.

[8] L. Hörmander, Analysis of Linear Partial Differential Operators, Vol. III, Springer-Verlag, (1983).

[9] T. Hosono and S. Kawashima, Decay property of regularity-loss type and application to some nonlinear hyperbolic-elliptic system, Math. Models Meth. Appl. Sci., 16 (2006),1839-1859.

[10] K. Ide and S. Kawashima, Decay property of regularity-loss type and nonlinear effects for dissipative Timoshenko system, Math. Models Meth. Appl. Sci., 18 (2008), 1001-1025.

[11] H. J. Lee, Uniform decay for solution of the plate equation with a boundary condition of memory type, Trends in Math, 9 (2006), 51-55.

[12] Y. Liu, Decay of solutions to an inertial model for a semilinear plate equation with memory, J. Math. Anal. Appl., 394 (2012), 616-632.

[13] [Y. Liu and S. Kawashima, Global existence and asymptotic behavior of solutions for quasi-linear dissipative plate equation, Discrete Contin. Dyn. Syst., 29 (2011), 1113-1139.

[14] [Y. Liu and S. Kawashima, Global existence and decay of solutions for a quasi-linear dissipative plate equation, J. Hyperbolic Differential Equations, 8 (2011), 591-614.

[15] Y. Liu and S. Kawashima, Decay property for a plate equation with memory-type dissipation, Kinet. Relat. Mod., 4 (2011), 531-547.

[16] S. Mao and Y. Liu, Decay of solutions to generalized plate type equations with memory,Kinet. Relat. Mod., 7 (2014), 121-131.

[17] S. Mao and Y. Liu, Decay properties for solutions to plate type equations with variable coefficients, Kinet. Relat. Mod., 10 (2017), 785-797.16

[18] N. Mori and S. Kawashima, Decay property for the Timoshenko system with Fourier's type heat conduction, J. Hyperbolic Differential Equations, 11 (2014), 135-157.

[19] N. Mori and S. Kawashima, Decay property of the Timoshenko-Cattaneo system, Anal.Appl., (2015), 1-21.

[20] N. Mori, J. Xu and S. Kawashima, Global existence and optimal decay rates for the Timoshenko system: The case of equal wave speeds, J. Differ. Equations., 258 (2015),1494-1518.

[21] M. Reed, and B. Simon, Methods of Modern Mathematical Physics, Vol. I, Academic Press, New York, (1975).

[22] J. E. Mu˜ noz Rivera, M.G. Naso and F.M. Vegni, Asymptotic behavior of the energy for a class of weakly dissipative second-order systems with memory, J. Math. Anal. Appl.,286 (2003), 692-704.

[23] Y. Sugitani and S. Kawashima, Decay estimates of solutions to a semi-linear dissipative plate equation, J. Hyperbolic Differential Equations, 7 (2010), 471-501.

[24] J. Xu, N. Mori and S. Kawashima, Global existence and minimal decay regularity for the Timoshenko system: The case of non-equal wave speeds, J. Differ. Equations., 259(2015), 5533-5553.

International Journal of Computer Applications Technology and Research
Volume 7–Issue 07, 270-273, 2018, ISSN:-2319–8656

Comparative analysis on Void Node Removal Routing algorithms for Underwater Wireless Sensor Networks

Mukhtiar Ahmed
Quaid-e-Awam University, of Science and Technology, Nawabshah, Sindh, Pakistan

Fauzia Talpur,
Department of Computer Science, Faculty of Computing
UTM, Malaysia

M.Ali Soomro
Quaid-e-Awam University, of Science and Technology, Nawabshah, Sindh, Pakistan

Abstract: The designing of routing algorithms faces many challenges in underwater environment like: propagation delay, acoustic channel behaviour, limited bandwidth, high bit error rate, limited battery power, underwater pressure, node mobility, localization 3D deployment, and underwater obstacles (voids). This paper focuses the underwater voids which affects the overall performance of the entire network. The majority of the researchers have used the better approaches for removal of voids through alternate path selection mechanism but still research needs improvement. This paper also focuses the architecture and its operation through merits and demerits of the existing algorithms. This research article further focuses the analytical method of the performance analysis of existing algorithms through which we found the better approach for removal of voids.
Keywords: Deployment; voids; water-current; v-shape; depth-adjustment; harsh

1. INTRODUCTION

In underwater environment the void node removal is one of the major issues which reduce the packets success ratio. The underwater obstacles and depletion of node energy creates the void node along the active packets forwarding path [1-3]. A number of factors individually or a combination of them, caused the void phenomena, such as sparse topology, temporary obstacles, and unreliable nodes or links [4, 5]. Existing relevant routing algorithms based on void node removal are briefly discussed.

2. RELATED WORK

Reliable and Energy Balanced Routing Algorithm (REBAR) is proposed by Chen, et al. [6]. In REBAR the two energy models are used to reduce the energy consumption of the ordinary sensor node; one is sphere energy depletion and other is extended energy depletion. REBAR is location based routing protocol, in REBAR the center sink node is placed on water surface, and sensor nodes are deployed in underwater. In REBAR data forwarding mechanism is based on hop-by-hop and transmission range R is fixed between sensor nodes. REBAR is based on the size of broadcast which is the stern alarm of REBAR which consumes the high energy. With high broadcast the more energy will be consumed by sensor nodes and with low broadcast size less energy will be consumed; with these both issues the REBAR keeps the balanced broadcast size mechanism to balance the energy level of the sensor node. In REBAR the distance d and vector v are the parameters which are stored in the packets format for calculating the routing direction with distance and vector between source and sink node for data forwarding. The packets information in REBAR is stored in the buffer of every node and on arrival of duplicate packets the node will drop the duplicate packets. The threshold value is used in between source and sink node to ensure the packets forwarding mechanism with right direction. For removal of void regions the boundary-set and non-boundary set mechanisms are adapted, with boundary set the information will be shared by the nodes for the presence of the void regions and alternate path selection mechanism will be adapted for data forwarding. In non-boundary set mechanism the data forwarding mechanism behaves normally [6]. REBAR focuses the data delivery ratio increases with respect to node movement but in real scenario the enhancement of data delivery ratio is not possible because the nodes behavior in underwater environment is not controllable. Horizontal and vertical node movement methodology is not clearly defined; so obviously packets drop ratio increases and results into the reduction of the overall network throughput. Removal of void regions are just hypothesis and this may also reduce the data delivery ratio.

Vector-Based Void Avoidance (VBVA) routing protocol is proposed by Xie, et al. [7]. VBVA functionality is adapted from VBF with variations for removal of void regions. For removal of void regions the VBVA adapted two mechanisms one is vector-shift and other is back-pressure. Void node can be detected by considering the example as shown in Figure 1(a); S is source node and D is destination node. If S and T are the start and end points then (ST) $\vec{}$ is the forwarding vector of the packets. The nodes K, L, and P are advances nodes on the forwarding vector and are denoted by AK, AL, and AP respectively. The nodes have property to detect the presence of a void to listen in the transmission of the packets by its neighbor nodes. The nodes also have a property to record the position information of the forwarding node. In Figure 1(a) the K and L have smaller advances than P on forwarding vector(ST) $\vec{}$. Node P has a larger advance among the neighbor nodes within the forwarding pipe and it concludes that it is a void node. Node P detects the void on a current forwarding vector and tries to bypass the void by changing the forwarding vector of the packets through the alternate route. To bypass the void through alternate route the node P can adapt vector-shift and back-pressure for removal of void region. In vector-shift mechanism the boundary of convex void by shift technique is adapted for data forwarding.

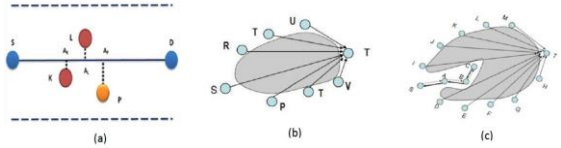

Figure 1: (a)Void node detection mechanism, (b) Vector shift, (c) Back pressure [7]

In Figure 1(b) the dashed area is void area whereas S is sender node and T is destination node. Data forwarding mechanism starts from S to T along vector (ST) $\vec{}$ if neighbor nodes of S like: P and R are not within the range in forwarding pipe then no forwarding mechanism will be considered. During the transmission mechanism if sender node S is unable to hear any movement from the acoustic channel than S node will consider the occurrence of void region and node S will forward the vector-shift control packet to the neighbor nodes to change the current forwarding vector position. In Figure 1(c) the shadow area is the concave void and node S is sender node whereas node T is sink node. If node S forwards the packets to node C and C is unable to forward the packets then node C will broadcast the back-pressure control packet to node B. Node B will also broadcast the back-pressure control packet to route the packet for node A. Node A will broadcast for node S, finally node S will shift the forwarding vector to node (HT) $\vec{}$ and (DT) $\vec{}$. The vector-shift mechanism is used to forward the packets towards sink node. The continuous node movement affects the performance of VBVA because through continuous movement node may away from the virtual pipe and will drop the packets. VBVA has adapted the vector-shift and back-pressure mechanisms without any consideration of the underwater parameters which shows that the authors have just focused the hypothesis. It is also observed that the performance evaluation of the VBVA is only based on VBF.

Hydraulic Pressure Based Any cast Routing (HydroCast) is proposed by [8]. Distributed localization HydroCast is geographic routing. The measured pressure mechanism is used by HydroCast for data forwarding to surface buoys. HydroCast resolves the issues of DBR routing protocol. The depth information with relevant clusters is adapted in HydroCast through pressure levels. The clusters formation mechanism of HydroCast is based on terminal nodes. The cluster formation mechanism is based on calculation of maximum progressive nodes which are nearer to destination nodes. Maximum progressive node plays a vital role in data forwarding mechanism and it has higher priority as compare to other neighbor nodes. For data forwarding the short time-out period is set by HydroCast. Limited flooding approach is used by HydroCast through maximum recovery technique. Flooding mechanism uses the performer or local maximum node for data forwarding. In HydroCast for local maximum node identification the tetra horizontal method is used. The data forwarding mechanism has been adapted between local maximum nodes through limited number of hops. For removal of void regions the greedy approach is used. The multiple numbers of data packets are received by sink node increases the extra burden on network. The energy efficient parameter in HydroCast is not clearly defined.

Depth Controlled Routing (DCR) proposed by Coutinho, et al. [9] is based on centralized algorithm to overcome the communication void problem. The algorithm determines which node become failing in greedy geographic forwarding task and then will calculate the new depth for possible routing. DCR is topology control geographic routing that considers the node mobility to adjust its depth, guaranteeing connectivity and eliminating communication void regions. In DCR the sensor nodes sense the underwater environment and periodically send the collected data towards sonobuoys. The distance of neighbors is considered to its nearest sonobuoys, obtained from beacons in the process of next-hop selection. Thus the neighbor that will be selected to act as a next-hop in the forwarding process is the node which is closest to some sonobuoys among all neighbors. If the selected node to act as next-hop cannot continue with greedy forwarding; it broadcast message to inform its neighbors for its void node situation. The neighbors then update its routing table, removing its void node entry. DCR faces some serious problems like: in sparse area the performance of DCR is reduced. The water pressure and water current affects the forwarder node along active path. No any proper mechanism is defined for removal of void node by DCR.

Void-Aware Pressure Routing (VARP) is proposed by Noh, et al. [10] which uses the local opportunist directional forwarding for data success ratio even in presence of voids. It uses the soft-state breadcrumb approach for mobile networks. It is based on enhanced beaconing and opportunist directional data forwarding. The V-shape architecture for data forwarding and in V-shape if any void region occurs is called trap area. If trap area appears the packets will be forwarded towards the new route through next-hop forwarding mechanism. It is observed that when nodes become spars the performance of VARP become slow due to affected of V-shape by underwater pressure. In VARP, the depth controlling mechanism is also not defined by authors.

Geographic Depth Adjustment Routing (GEDAR) is proposed by Coutinho, et al. [11] which is based on depth adjustment topology controlling mechanism for removal of void nodes. It moves the void node in new depth with greedy forwarding strategy. The sea swarm architecture is adapted for packets forwarding. The sensor nodes are equipped with buoyancy-based depth adjustment which adjusts the depth of the sensor nodes in underwater. The depth adjustment mechanism for sensor node location information is based on vertical movement, energy cost values and periodic beaconing. The data packets are forwarded by qualified neighbor node through next-hop forwarder mechanism from source to sink. During packets forwarding mechanism each node will observe the void node and if void node appears during packets forwarding the void node will be shifted towards new depth through greedy forwarding mechanism with two-hop steps. The topology control mechanism defined by GEDAR is not so easy due to water pressure and continuous node movement. The depth calculation mechanism is not properly defined by proposed algorithm.

Opportunist Void Avoidance Routing (OVAR) is proposed by Ghoreyshi, et al. [12] which use the prioritizing the group of candidate nodes with highest packets advancement mechanism. Given the density of neighbor nodes, each forwarding node is able to hold a trade-off between packet advancement and energy consumption by adjusting the number of nodes in its forwarding set. OVAR is also able to select the forwarding set in any direction from the sender without including any hidden node. The operation of OVAR is based on four phases. In first phase an adjacency graph is constructed at every node and using a heuristic some clusters i.e clique sub-graphs is created to ensure that hidden nodes are removed from forwarding sets. In second phase the best forwarding set is selected using expected packets advancement to maximize the chance of successful delivery of packets. In third phase the number of forwarding nodes in the forwarding set is adjusted to make a trade-off between reliability and energy consumption. In fourth phase the holding time is calculated at each candidate node before the forwarding node. In OVAR the removal of void node

mechanism is not properly defined, if any node becomes as a void node due to underwater obstacles and that node is the packets forwarder node then that node will drop the packets and will reduce the data success ratio.

Void Handling Geo-Opportunist Routing (VHGOR) proposed by Kanthimathi [13] is based on quick hull algorithm for convex or concave voids. When the node approaches a convex void; reconstruction of convex hull helps to determine an alternative way to resume the greedy forwarding if the neighbor within its proximity. Failure of convex void handling during communication void makes VHGOR switch to concave void handling or recovery mode to recover the packets from local maximum node and route the packets towards destination. For convex void handling the immediate forwarder node will sent back ACK to source node within some certain time period; if ACK not received by source node means forwarder node is in void region and VHGOR will manage the alternate route to forward packets through convex hull. During creation of void node; if convex hull will not to be built then VHGOR consider the concave hull or recovery mode. In concave hull the packets are re-routing along the recovery path. The recovery path works from down-stream to upstream to route packets towards destination from alternative paths. VHGOR has adapted the void problem from VBVA and VHGOR is failure to calculate the water depth from sea surface to bottom. No proper node mobility model is defined for controlling of node movement. The multi-hop technique from top to seabed is used; so due to long distance multi-hop technique cannot shows the better results for data success rate and also maximizes the end-to-end delay.

3. PERFORMANCE ANALYSIS

In Table 1, the parametric performance analysis of void node removal routing algorithms are shown. The void node removal is based on: node mobility controlled, hop-by-hop/end-to-end delay, single/multiple sink, multipath, hello/control packet, and void node removal technique. The analysis is based on protocol operation with packets forwarding mechanism.

4. CONCLUSION

Void node removal means the node which may come in underwater obstacles or the node may become dead due to energy depletion. Almost the existing routing algorithms focuses the underwater obstacle and when node becomes void, the node may drop the packets and will affect the overall performance of the network. The REBAR routing algorithm is based on boundary set mechanism to remove the void but it is observed that boundary set approach is not suitable for underwater environment. In same way the HydroCast is based on flooding mechanism for removal of voids, the approach used by Hydrocast is not mentioned in its research paper that how it forwards the packets when node becomes void. From the aforementioned void node algorithms the quick-hull and depth-adjustment mechanisms used by VHGOR and GEDAR are observed the best approaches for removal of voids from underwater environment.

Table 1: Parametric performance analysis of void node removal routing

S_No	Routing Protocol	Year	Node mobility Controlled	Hop-by-hop/end-to-end	Single/ Multiple Sink	Multipath	Hello/ Control Packet	Void Node removal technique
1.	REBAR	2008	√	hop-by-hop	Single-sink	×	×	Boundary set
2.	VBVA	2009	×	end-to-end	Single-sink	×	√	Vector shift & back-pressure
3.	HydroCast	2010	×	hop-by-hop	Multi-sink	×	×	Hop-limited 2D flooding
4.	DCR	2013	√	hop-by-hop	Single-sink	×	×	Depth-controlled
5.	VARP	2013	√	hop-by-hop	Single-sink	√	√	V-shaped trapped area
6.	GEDAR	2016	√	hop-by-hop	Multi-sink	v	×	Recovery mode based on depth-adjustment
7.	OVAR	2016	×	hop-by-hop	Single-sink	v	×	Opportunist void avoidance
8.	VHGOR	2017	√	hop-by-hop	Single-sink	v	×	Quick hull algorithm

5. REFERENCES

[1] R. H. Rahman, C. Benson, and M. Frater, "Routing Protocols for Underwater Ad Hoc Networks," Oceans, 2012, IEEE Conference, Yeosu-si, Jeollanam-do, South Korea, 2012.

[2] Y. Wang, Y. J. Liu, and Z. W. Guo, "Three-dimensional ocean sensor networks: A survey," Journal of Ocean University of China, vol. 11, pp. 436-450, Dec 2012.

[3] P. Casari and M. Zorzi, "Protocol design issues in underwater acoustic networks," Computer Communications, vol. 34, pp. 2013-2025, Nov 2011.

[4] M. Xu, G. Z. Liu, H. F. Wu, and W. Sun, "Towards Robust Routing in Three-Dimensional Underwater Wireless Sensor Networks," International Journal of Distributed Sensor Networks, vol. 9, pp. 1-15, 2013.

[5] S. M. Ghoreyshi, A. Shahrabi, and T. Boutaleb, "Void-Handling Techniques for Routing Protocols in Underwater Sensor Networks: Survey and Challenges," IEEE Communications Surveys & Tutorials, vol. 19, pp. 800-827, 2017.

[6] J. M. Chen, X. B. Wu, and G. H. Chen, "REBAR: A Reliable and Energy Balanced Routing Algorithm for UWSNs," In Grid and Cooperative Computing, 2008, GCC'08. Seventh International conference on. IEEE, vol. Shenzhen, China, pp. 349-355, 2008.

[7] P. Xie, Z. Zhou, Z. Peng, J.-H. Cui, and Z. Shi, "Void avoidance in three-dimensional mobile underwater sensor networks," in Wireless Algorithms, Systems, and Applications, ed: Springer, Springer, Berlin, Heidelberg, 2009, pp. 305-314.

[8] U. Lee, P. Wang, Y. Noh, F. Vieira, M. Gerla, and J.-H. Cui, "Pressure routing for underwater sensor networks," in INFOCOM, 2010 Proceedings IEEE, San Diego, Calif, USA, 2010, pp. 1-9.

[9] R. W. Coutinho, L. F. Vieira, and A. A. Loureiro, "DCR: Depth-Controlled routing protocol for underwater sensor networks," in Computers and Communications (ISCC), 2013 IEEE Symposium on, Split, Croatia, 2013, pp. 000453-000458.

[10] Y. Noh, U. Lee, P. Wang, B. S. C. Choi, and M. Gerla, "VAPR: void-aware pressure routing for underwater sensor networks," IEEE Transactions on Mobile Computing, vol. 12, pp. 895-908, 2013.

[11] R. W. Coutinho, A. Boukerche, L. F. Vieira, and A. A. Loureiro, "Geographic and opportunistic routing for underwater sensor networks," IEEE Transactions on Computers, vol. 65, pp. 548-561, 2016.

[12] S. M. Ghoreyshi, A. Shahrabi, and T. Boutaleb, "An opportunistic void avoidance routing protocol for underwater sensor networks," in Advanced Information Networking and Applications (AINA), 2016 IEEE 30th International Conference on, Lens, Switzerland, 2016, pp. 316-323.

[13] N. Kanthimathi, "Void handling using Geo-Opportunistic Routing in underwater wireless sensor networks," Computers & Electrical Engineering, vol. 127, pp. 1-15, 2017.

[14] B. Karp and H.-T. Kung, "GPSR: Greedy perimeter stateless routing for wireless networks," in Proceedings of the 6th annual international conference on Mobile computing and networking, ACM,, Boston, MA, USA, 2000, pp. 243-254.

[15] F. Zhou, G. Trajcevski, R. Tamassia, B. Avci, A. Khokhar, and P. Scheuermann, "Bypassing holes in sensor networks: Load-balance vs. latency," Ad Hoc Networks, vol. 61, pp. 16-32, 2017.

International Journal of Computer Applications Technology and Research
Volume 7–Issue 07, 274-277, 2018, ISSN:-2319–8656

Survey on Energy-Efficient Routing Algorithms for Underwater Wireless Sensor Network

Mukhtiar Ahmed
Quaid-e-Awam University,
of Science and Technology,
Nawabshah, Sindh, Pakistan

Fauzia Talpur,
Department of Computer
Science, Faculty of Computing
UTM, Malaysia

M.Ali Soomro
Quaid-e-Awam University,
of Science and Technology,
Nawabshah, Sindh, Pakistan

Abstract: In underwater environment, for retrieval of information the routing mechanism is used. In routing mechanism there are three to four types of nodes are used, one is sink node which is deployed on the water surface and can collect the information, courier/super/AUV or dolphin powerful nodes are deployed in the middle of the water for forwarding the packets, ordinary nodes are also forwarder nodes which can be deployed from bottom to surface of the water and source nodes are deployed at the seabed which can extract the valuable information from the bottom of the sea. In underwater environment the battery power of the nodes is limited and that power can be enhanced through better selection of the routing algorithm. This paper focuses the energy-efficient routing algorithms for their routing mechanisms to prolong the battery power of the nodes. This paper also focuses the performance analysis of the energy-efficient algorithms under which we can examine the better performance of the route selection mechanism which can prolong the battery power of the node.

Keywords: super node; dolphin node; acoustic channel; data packets; forwarder node; ordinary node

1. INTRODUCTION

The underwater equipment such as underwater sensor nodes, Acoustic Underwater Vehicles (AUVs) and underwater modems with acoustic channel have made communication possible in the underwater environment. Sensor nodes are able to transmit the data packets with their sensing capabilities within the short distance [1-3]. The underwater sensor nodes are composed of sensing unit, acoustic modem, processing unit, communication unit and power unit. The sensing unit measures the physical conditions like water temperature and water pressure. The acoustic modem is responsible to convert the RF signal into acoustic signaling while processing unit is responsible to process the data and converting it into the required signaling form [4] . The communication unit is used to transfer the data to the acoustic modem. All the discussed units' runs under the power unit, power unit is responsible to supply the required energy to all these units to perform functionality of the node. The nodes in underwater environment have ability to communicate between each other or to communicate with surface nodes through acoustic channel [5]. Majority of the researchers have given feasible algorithms, deployment methodologies, different architectural structures as well as data forwarding mechanisms to prolong the battery life of the nodes; but due to the underwater environmental conditions and some delay factors, the underwater nodes cannot maintain their power levels and the power supply deplete earlier [6]. Following are the energy-aware routing protocols described with advantages and drawbacks.

2. RELATED WORK

Delay-tolerant Data Dolphin (DDD) is an energy efficient routing algorithm proposed by Magistretti, et al. [7]. DDD is for the delay tolerant applications. The DDD routing algorithm is based on collector nodes called dolphin and stationary nodes; the dolphin nodes harvest the information sensed by the stationary nodes. The routing algorithm eliminates the energy expensive multi-hop communication. The stationary nodes are responsible to transmit its collected data to the nearest in the range of dolphins. The stationary nodes are deployed on sea bed area of interest. The authors have used the two components of the acoustic channel one is communication component and other is transceivers component for data forwarding. Through communication component the dolphin node is able to communicate and through transceivers component the presence of dolphin node is analyzed through beacon signal. The dolphin node forwards the collected packets to the base station which are deployed on water surface. In DDD the random movement of dolphin nodes will not able to collect all the data packets from the sensor nodes and in resultant the data delivery ratio will be degraded. In DDD; if the number of dolphins increases the overall cost of the network will also be increased.

Power-Efficient Routing (PER) proposed by Huang, et al. [8]. PER routing enhances the battery power of the sensor node. PER algorithm is based on two modules one is forwarder node selector and other is forwarding tree trimming. In PER the fuzzy logic system and decision trees based mechanisms are used for forwarder node selector, the forwarder node selection mechanism may be affected due to the water pressure and may reduce the data delivery ratio of PER. If forwarder node will come in the void region then it will drop the packets continuously and will die earlier.

Energy Efficient Depth Based Routing (EEDBR) is proposed by Wahid et al. [9]. EEDBR protocol is based on knowledge acquisition and data forwarding phases. In EEDBR ordinary sensor nodes are placed from top to bottom of the water and sink nodes are placed on water surface and source nodes are placed at bottom of the water. In EEDBR from sink nodes to onshore data center the radio signaling are used whereas in underwater the acoustic signaling is used. In knowledge acquisition phase the Hello message is forwarded between sensor nodes and neighbor nodes the nodes which keep smaller depth Id may involve for data forwarding. In data forwarding mechanism the depth and residual energy parameters are considered. The nodes which keep high energy with smaller depth are only involved in data forwarding. The depth calculation mechanism adapted by authors is failure in

sparse area network. No any proper algorithm is given by EEDBR for balanced energy consumption.

Energy efficient Mobicast routing protocol is proposed by Chen and Lin [10]. The Mobicast is power-saving 3D routing protocol which overcomes the problem of unpredictable 3D holes. In Mobicast the "apple peel" is proposed to resolve the problem of unpredictable 3D holes. The architecture of Mobicast is based on underwater sensor nodes which are deployed randomly in 3D area of water around the Autonomous Underwater Vehicles (AUV) in form of 3D zone of reference or 3D ZOR as shown in Figure 1 and Figure 2. The AUV travels along the user defined path and collects the information from the sensor nodes within different time intervals of 3D ZORs. The sleep and active nodes are used to resolve the problem of unpredictable holes. Active nodes are responsible to forward the sensed data to the AUV. Mobicast uses the geographic 3D Zone of Relevance (3D ZOR3) and 3D Zone of Forwarding (3D ZOF) which are created by AUV at time t to indicate which sensor node should forward the sensed data to the AUV as shown in Figure 1 and Figure 2. Fully distributed algorithm is used by Mobicast which reduces the power consumption of the sensor nodes and the message overheads. Mobicast enhances the data delivery ratio. In Mobicast, the creation of user defined route in underwater 3D environment is very hard due to the water pressure. Due to the continuous water movement if the active nodes may remain away from the AUV then the active nodes can drop the packets and ultimately the packets delivery ratio will be reduced.

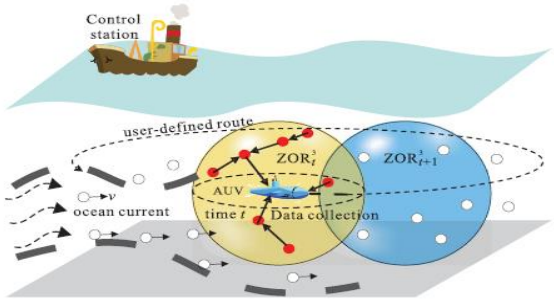

Figure 1: AUV collects data from sensor nodes with ⟦ZOR⟧_t^3 with time t [10]

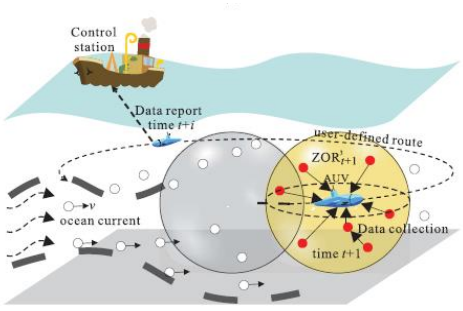

Figure 2: AUV collects data from sensor nodes with ⟦ZOR⟧_t^3 with time t+1 [10]

Link-state Adaptive Feedback Routing (LAFR) algorithm is proposed by Zhang, et al. [11]. LAFR is energy efficient routing algorithm based on asymmetric link mechanism. The data forwarding mechanism is based on beam width with communication range up to 3600 angle. The complicated mechanism for data forwarding with calculation of angle will put the heavy load on ordinary sensor node; due to this network load the sensor node will die earlier and average energy consumption of LAFR will be increases.

Multi-layer Routing Protocol (MRP) is proposed by Wahid, et al. [12]. MRP routing protocol is used to resolve the problem of localization and enhances the battery life of ordinary sensor node. The network architecture is based on sink nodes, super nodes and sensor nodes. The sink nodes are placed on the water surface and super nodes are fixed and spread in different water levels. Sensor nodes are deployed at the bottom of the water. MRP develops the 2D layers around the super node. For packets forwarding the layer ID and sensor node ID with different power levels are proposed, the creation of layers are shown in Figure 3. The authors claimed that the super node is used to enhance the battery life of ordinary sensor nodes. MRP uses the 2D node deployment mechanism but underwater supports 3D deployment. In MRP the packets holding time algorithm is not properly defined. If sensor node may remain away from super node then the sensor node may drop the packets and ultimately the packets delivery ratio might be affected.

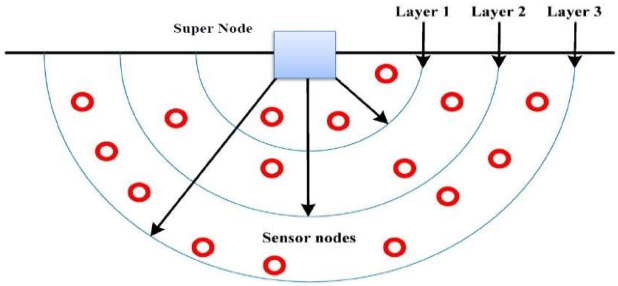

Figure 3: Formation of different layers around super node [12]

Energy Efficient Depth Based Routing (EE-DBR) is proposed by Diao, et al. [13] which prolongs the battery life of the sensor node through reducing of multipath redundancy forwarding mechanism. The ToA ranging technique is used to measure distance between sensor nodes. If measured distance increases the node will stop the packets forwarding and can save its energy. ToA with measured distance technique of EE-DBR controls the data packets on a fixed range data forwarding route, if distance increases from source to sink node the ToA with measured distance technique will enhance the end-to-end delay.

Reliable and Energy Efficient Protocol (REEP) is proposed by Rahman, et al. [14] which utilizes the Time of Arrival (ToA) algorithms as described by Diao, et al. [13] to find the node distance to its respective sink. REEP utilizes the ToA information to find best available routing path. A REEP operation is based on two phases one is network setup phase and other is data transmission phase. In network setup phase the sink nodes are deployed on water surface whereas ordinary nodes are deployed in underwater. In network phase forwarder node selection is based on node location information and node residual energy. In REEP the ToA arrival technique is used to find the approximately distance between sender and receiver nodes. The three kind of packets format are used to develop the route for packets forwarding:

one is hello packet format, second is reply packet format, and third is data packet format. In data transmission phase data packets are forwarded through multi-hop with calculated distance from source to destination. The REEP packets forwarding functionality is based only on vertical modem; if majority number of nodes become sparse the distance calculation mechanism of REEP will become failure and nodes will drop the packets continuously and will lose their energy.

Energy-efficient Multipath Grid-based Geographic Routing (EMGGR) is proposed by Al Salti, et al. [15]. EMGGR is position based routing algorithm and is consists of 3D logical grid multipath approach. The EMGGR refers the three phases one is gateway election mechanism, second is updating gateways' information mechanism, and third is packets forwarding mechanism. EMGGR considers the geographic area of the network with 3D logical grid partitions. EMGGR considers the deployment of every sensor node with the single cell from the logical grid with xyz addressing mechanism and presumes that every sensor node is well aware about its location through built-in localization service. EMGGR is based on multipath route selection from source to virtual cell gateway node and virtual cells gateway nodes are responsible to relay the data packets to the surface sink node. The algorithm is based on single sink node only.

Energy-efficient Distance Routing Protocol (DRP) proposed by Chao, et al. [16] considers the distance-varied collision probability for route selection with residual energy of each node. DRP is based on smaller and larger vulnerability range between nodes through inner and outer radius. In DRP the sink node broadcast HELLO packets periodically to the neighbor nodes and the best forwarder node can be selected through its residual energy. In DRP the multipath node disjoint route is developed between sink and source nodes through forwarder nodes. In DRP if the number of nodes increases the performance of entire network is reduces due collision probability. In DRP if the distance will increase due to mobile node then forwarder node will drop the packets and will die earlier.

3. PERFORMANCE ANALYSIS

In Table 1, the parametric performance analysis of the energy efficient routing algorithms is shown, the performance parameters are selected from the architecture and operation of the energy efficient routing algorithms. The parameters for measuring the performance of the energy efficient routing algorithms are: single/multiple copies, hop-by-hop/end-to-end, single/multiple sink, multipath, hello/control packet, and requirements/assumptions

Table 1: Performance analysis of routing algorithms based on energy efficiency

S_No	Routing Protocol	Year	Single/Multiple copies	Hop-by-hop/end-to-end	Single/ Multiple Sink	Multipath	Hello/Control Packet	Requirement and Assumptions
1.	DDD	2007	Single-copy	Single hop	n/a	×	yes	Network with special setup
2.	PER	2010	Single-copy	Hop-by-hop	Single-sink	√	yes	Geo. location information
3.	EEDBR	2011	Multiple-copies	Hop-by-hop	Multi-sink	√	yes	Depth information
4.	Mobicast	2013	Multiple-copies	Hop-by-hop	Single-sink	√	no	Depth information
5.	LAFR	2013	Single-copy	End-to-end	Single-sink	√	no	n/a
6.	MRP	2014	Multiple-copies	Hop-by-hop	Multi-sink	√	yes	Depth information
7.	EE-DBR	2015	Single-copy	Hop-by-hop	Single-sink	√	no	Depth directional information
8.	REEP	2015	Single-copy	End-to-end	Single-sink	×	yes	Depth information
9.	EMGGR	2016	Single-copy	Hop-by-hop	Single-sink	√	no	Depth information
10.	DRP	2017	Single-copy	Hop-by-hop	Multi-sink	√	yes	Depth information

4. CONCLUSION

Energy-efficient routing algorithms as mentioned above are based to prolong the battery power of the sensor nodes, DDD algorithm has used the dolphin node to save the power of the nodes, PER algorithm has used the fuzzy logic and decision tree approach to prolong the battery power of the node, EEDBR saves the energy of the nodes through forwarder node selection and residual energy selection mechanism, Mobicast

prolong the battery power of the node through AUV. LAFR routing algorithm prolong the battery power of the node through asymmetric link selection mechanism, MRP prolongs the battery power of the node through layer-formation and super node selection mechanism. EE-DBR is based on distance selection and ToA arrival which saves the power of the ordinary node. From aforementioned algorithms the EMGGR algorithm uses the 3D grid approach with multipath selection mechanism which is the better approach to prolong the battery power of the nodes as compare to other defined algorithms.

REFERENCES

[1] M. Ahmed and M. Salleh, "Localization schemes in Underwater Sensor Network (UWSN): A Survey," *Indonesian Journal of Electrical Engineering and Computer Science.*, vol. 1, pp. 119-125, 2015.

[2] M. Z. Abbas, K. A. Bakar, M. A. Arshad, M. Tayyab, and M. H. Mohamed, "Scalable Nodes Deployment Algorithm for the Monitoring of Underwater Pipeline," *TELKOMNIKA (Telecommunication Computing Electronics and Control)*, vol. 14, pp. 1183-1191, 2016.

[3] N. Bahrami, N. H. H. Khamis, A. Baharom, and A. Yahya, "Underwater Channel Characterization to Design Wireless Sensor Network by Bellhop," *TELKOMNIKA (Telecommunication Computing Electronics and Control)*, vol. 14, pp. 110-118, 2016.

[4] M. Ahmed, M. Salleh, and M. I. Channa, "Critical Analysis of Data Forwarding Routing Protocols Based on Single path for UWSN," *International Journal of Electrical and Computer Engineering*, vol. 6, pp. 1695-1701, 2016.

[5] G. Han, J. Jiang, N. Bao, L. Wan, and M. Guizani, "Routing protocols for underwater wireless sensor networks," *Communications Magazine, IEEE*, vol. 53, pp. 72-78, 2015.

[6] N. Li, J.-F. Martínez, J. M. Meneses Chaus, and M. Eckert, "A Survey on Underwater Acoustic Sensor Network Routing Protocols," *Sensors*, vol. 16, p. 414, 2016.

[7] E. Magistretti, J. Kong, U. Lee, M. Gerla, P. Bellavista, and A. Corradi, "A mobile delay-tolerant approach to long-term energy-efficient underwater sensor networking," in *Wireless Communications and Networking Conference, 2007. WCNC 2007. IEEE*, Sheraton Hotel, Hong Kong, 2007, pp. 2866-2871.

[8] C. J. Huang, Y. W. Wang, H. H. Liao, C. F. Lin, K. W. Hu, and T. Y. Chang, "A power-efficient routing protocol for underwater wireless sensor networks," *Applied Soft Computing*, vol. 11, pp. 2348-2355, Mar 2011.

[9] A. Wahid, S. Lee, H. J. Jeong, and D. Kim, "EEDBR: Energy-Efficient Depth-Based Routing Protocol for Underwater Wireless Sensor Networks," *Advanced Computer Science and Information Technology*, vol. 195, pp. 223-234, 2011.

[10] Y.-S. Chen and Y.-W. Lin, "Mobicast routing protocol for underwater sensor networks," *Sensors Journal, IEEE*, vol. 13, pp. 737-749, 2013.

[11] S. Zhang, D. Li, and J. Chen, "A link-state based adaptive feedback routing for underwater acoustic sensor networks," *Sensors Journal, IEEE*, vol. 13, pp. 4402-4412, 2013.

[12] A. Wahid, S. Lee, D. Kim, and K. S. Lim, "MRP: A Localization-Free Multi-Layered Routing Protocol for Underwater Wireless Sensor Networks," *Wireless Personal Communications*, vol. 77, pp. 2997-3012, Aug 2014.

[13] B. Diao, Y. Xu, Z. An, F. Wang, and C. Li, "Improving Both Energy and Time Efficiency of Depth-Based Routing for Underwater Sensor Networks," *International Journal of Distributed Sensor Networks*, vol. 11, pp. 1-9, 2015.

[14] Z. Rahman, F. Hashim, M. Othman, and M. F. A. Rasid, "Reliable and energy efficient routing protocol (REEP) for underwater wireless sensor networks (UWSNs)," in *Communications (MICC), 2015 IEEE 12th Malaysia International Conference on, Kuching, Sarawak, Malaysia*, 2015, pp. 24-29.

[15] F. Al Salti, N. Alzeidi, and B. R. Arafeh, "EMGGR: an energy-efficient multipath grid-based geographic routing protocol for underwater wireless sensor networks," *Wireless Networks*, vol. 23, pp. 1301-1314, 2017.

[16] C. M. Chao, C. H. Jiang, and W. C. Li, "DRP: An energy-efficient routing protocol for underwater sensor networks," *International Journal of Communication Systems*, vol. 1, pp. 1-24, 2017.

International Journal of Computer Applications Technology and Research
Volume 7–Issue 07, 278-280, 2018, ISSN:-2319–8656

Application of 3D Printing in Education

Mr. Shrinath S Pai,
Research Scholar,
Jain University,
Bangalore
India

Mr. Gourish B,
Asst Professor,
Dept of Computer,
Shree Guru
Sudhindra BCA
College, Bhatkal
India

Ms. Pallavi Moger,
Student, Dept of CS,
Shree Guru
Sudhindra BCA
College, Bhatkal
India

Mr. Pavan Mahale,
Student, Dept of CS,
Shree Guru
Sudhindra BCA
College, Bhatkal
India

Abstract: This paper provides a review of literature concerning the application of 3D printing in the education system. The review identifies that 3D Printing is being applied across the Educational levels [1] as well as in Libraries, Laboratories, and Distance education systems. The review also finds that 3D Printing is being used to teach both students and trainers about 3D Printing and to develop 3D Printing skills.

Keywords: Education, 3DP, Education Application, School, Design

1. INTRODUCTION

3D Printing is a process for making a physical object from a three-dimensional digital model, typically by laying down many successive thin layers of a material. [2] It brings a digital object (its CAD representation) into its physical form by adding layer by layer of materials.

Even though 3D printers have been around for almost 30 years, the recent rise of low-cost printers has led some to proclaim the onset of a new industrial revolution. Schools and libraries all over the world are bringing these powerful tools to students in classrooms. [3]

For example, China is putting 3D printers in each of its 400,000 elementary schools. In the U.S., we are adding 3D printers into schools at a good rate, particularly into CAD programs, but also into traditional art and social studies classrooms and even business programs.

The result of bringing these tools into classrooms is a rekindling of the powerful pedagogy of hands-on learning, which was prevalent in American schools mid-twentieth century. As we will demonstrate, 3D printing leverages hands-on learning to deepen our educational approach to traditional academic subjects.

2. OVERVIEW / HISTORY

Although 3D printing is commonly thought of as a new ‘futuristic’ concept [4], it has actually been around for more than 30 years.

The earliest 3D printing technologies first became visible in the late 1980’s, at which time they were called Rapid Prototyping (RP) technologies. This is because the processes were originally conceived as a fast and more cost-effective method for creating prototypes for product development within industry.

3D Systems’ first commercial RP system, the SLA-1, was introduced in 1987 and following rigorous testing the first of these system was sold in 1988.

Throughout the 1990’s and early 2000’s a host of new technologies continued to be introduced.

In 2007, the market saw the first system under $10,000 from 3D Systems, but this never quite hit the mark that it was supposed to.

2012 was the year that alternative 3D printing processes were introduced at the entry level of the market.

3D printer sales have been growing ever since, and as additive manufacturing patents continue to expire, more innovations can be expected in the years to come.

3D Printing essentially describes a assortment of technologies that digitally formulate three dimensional objects on a preservative layer-by-layer basis. Its official classification of “additive manufacturing” (AM) is defined as “a process of joining materials to make objects from 3D model data, usually layer upon layer, as opposed to subtractive manufacturing methodologies”. [5]

3D Printing possesses a number of advantages relative to these processes. However, as an emerging technology, it is still in development; it has yet to fully realise its full performance and there are additional socioeconomic challenges to overcome based on the novelty of the technology.

The explosion in consumer 3D Printing originated with the RepRap project, an open source project to create a self-replicating robot. This project attracted significant interest globally from members of the Maker movement. The combination of this project and the rise of crowd funding platforms such as Kick starter and Indiego go has enabled numerous entrepreneurial ventures to launch onto the market.

3. 3D PRINTING

3D printers build objects using a process known as additive manufacturing. Material is put down in layers; each

layer adds to the previous layer and in turn becomes a base for the next layer. [6]

Most 3D printers in the consumer market use thermoplastic inks in the printing process. These polymers become soft and pliable within a temperature range and then re-solidify when allowed to cool.

Typical manufacturing techniques are known as 'Subtractive Manufacturing' such as Milling and Cutting. This type of process creates a lot of waste since; the material that is cut off generally cannot be used for anything else and is simply sent out as scrap.

3D Printing eliminates such waste since the material is placed in the location that it is needed only, the rest will be left out as empty space.

4. 3D Printing Application Areas

3-D printing is extremely enlarging its application areas. The capabilities of this 3 dimensional technology are growing rapidly with the market demands. Today, this technology has become a possible alternative to conventional manufacturing processes [7] in an increasing number of applications including engineering, automotive, medical, education, fashion and many more. The advantages of 3-D printing over traditional manufacturing methods have changed the way; many things are designed, developed, produced and tested.

3D Printing is currently used in following areas:

- Engineering
- Medical Sector
- Fashion Industry
- Landscaping & Sculpturing Services
- Education, Research & Development
- Automobile Engineering
- Aeronautical Engineering
- Robotics
- Construction Industry
- Environmental Conservation
- Specialty Materials
- 3D Bioprinting
- Bio-Organ printing
- Health Sector
- Dental implants
- Skull and jaw implants
- Security and integration

5. 3D Printing Application in Education

3D printing technology is a rising technology in universities, colleges and high schools. With this technology, teaching and learning process has changed drastically.[8] 3 dimensional printing is a revolutionary and innovative technology that brings with itself, new methods of learning and understanding concepts that were very difficult with the traditional methods.

3D Printing is widely used in Education Sector.

Chemistry: 3D Structures, Molecules, Organic Bonding, Elements construction

Mathematics: Create geometrical objects, shapes presentation.

Marketing: Sample Display Product, Chart, 3D Graphs

Sports Education: Blueprint of sports / games plan, Sample sports equipments.

Fashion Technology: Dress Material Design,

Pre-Schools: Training objects, Teaching Aids

Networking: Network Topology Design, Network Components Design

Aeronautical: Aerodynamics design, Solid Objects

Music Training: Musical Instrument Design (Demo)

Architecture: Building Design, Blueprint

History: Historical Object Design, Fossil & Monuments Design,

Food Technology: Food Sample Design, Food Making

Graphic Design: Design on 3D Objects, Learning Tools

Geography: Models, Map Design

Engineering: Drawing, Production Unit Sample Design

Biology: Cell Structure, Specimens

Advantages of 3D printers in Education, Research & Development:- [9]

- It gives the practical exposure to the participants.
- The blueprint of the object helps in understanding the real object.
- Students of architecture, fine arts or biomedicine can benefit from this state-of-the-art printing technology
- This 3D printing technology gives the students complete understanding of objects and structures
- Prototype design helps students in understanding subject.
- Students can give their digital data a physical appearance with this technology

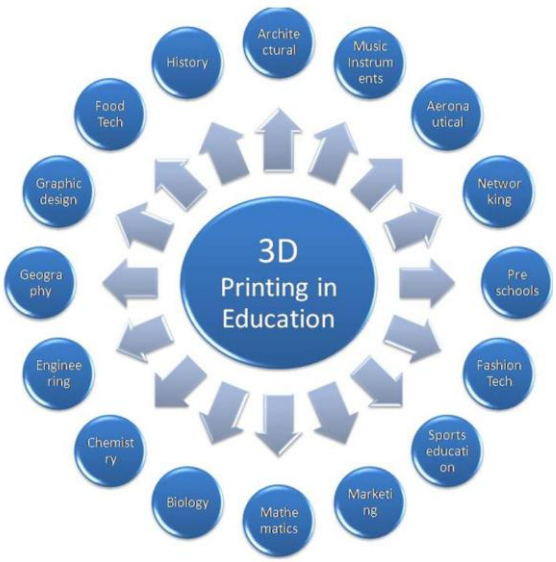

Conclusion

3D printing technology is a rising technology in universities, colleges and high schools. With this technology, teaching and learning process has changed drastically. 3 dimensional printing is a revolutionary

REFERENCES

[1] Simon Ford, Tim Minshall, 2016. 3D Printing in education: a literature review, version 1.0 .

[2] Igor Verner, Amir M, Digital Design and 3D Printing in technology teacher education, Procedia CIRP 36 (2015) 182-186.

[3] School News, The 3D Printing Revolution in Eucation, A new approach to learning in the 21st century.

[4] Kainant W, Hasnain A, Ovais H, Innovation in Education – Inclusion of 3D-Printing technology in Modern Education system, ISSN 2222-1735, Vol 8, No 1, 2017

[5] Alekos Pantazis, Christina Priavolou, 3D printing as a means of learning and communication: The 3Ducation project revisited, www.elsevier.com/locate/tele.

[6] Vasilis K, Vasilis N, Christos G, Open source 3D printing as a means of learning: An educational experiment in two high schools in Greece, Telematics and Informatics 32 (2015) 118–128

[7] Jennifer Loy, eLearning and eMaking: 3D Printing Blurring the Digital and the Physical, Educ. Sci. 2014, 4, 108-121; doi:10.3390/educsci4010108

[8] David Barlex, Making by printing – disruption inside and outside school?

[9] 3D Printer, Buyer's Guide, For Professional and Production Applications

International Journal of Computer Applications Technology and Research
Volume 7–Issue 07, 281-285, 2018, ISSN:-2319–8656

Hangul Recognition Using Support Vector Machine

Rahmatina Hidayati
Department of Electrical Engineering
University of Brawijaya
Malang, East Java, Indonesia

Moechammad Sarosa
Department of Electrical Engineering
State Polytechnic of Malang
Malang, East Java, Indonesia

Panca Mudjirahardjo
Department of Electrical Engineering
University of Brawijaya
Malang, East Java, Indonesia

Abstract: The recognition of Hangul Image is more difficult compared with that of Latin. It could be recognized from the structural arrangement. Hangul is arranged from two dimensions while Latin is only from the left to the right. The current research creates a system to convert Hangul image into Latin text in order to use it as a learning material on reading Hangul. In general, image recognition system is divided into three steps. The first step is preprocessing, which includes binarization, segmentation through connected component-labeling method, and thinning with Zhang Suen to decrease some pattern information. The second is receiving the feature from every single image, whose identification process is done through chain code method. The third is recognizing the process using Support Vector Machine (SVM) with some kernels. It works through letter image and Hangul word recognition. It consists of 34 letters, each of which has 15 different patterns. The whole patterns are 510, divided into 3 data scenarios. The highest result achieved is 94,7% using SVM kernel polynomial and radial basis function. The level of recognition result is influenced by many trained data. Whilst the recognition process of Hangul word applies to the type 2 Hangul word with 6 different patterns. The difference of these patterns appears from the change of the font type. The chosen fonts for data training are such as Batang, Dotum, Gaeul, Gulim, Malgun Gothic. Arial Unicode MS is used to test the data. The lowest accuracy is achieved through the use of SVM kernel radial basis function, which is 69%. The same result, 72 %, is given by the SVM kernel linear and polynomial.

Keywords: Support Vector Machine; SVM; Kernel Polynomial; Kernel Linear; Kernel Radial Basis Function; Hangul

1. INTRODUCTION

Optical Character Recognition (OCR) is a character introduction system with images input. It contains texts that would be converted to the edited versions[1]. The work of OCR system depends on the kind of processed text. Generally, the text is divided into three categories. They are written, printed, and typed text[2].

Some researches on OCR System have been conducted. One of methods ever used is Support Vector Machine (SVM). A kind of character which had ever been searched by using SVM is Hindi number, which is known as Numeral Kanada, upper case and lower case alphabet A-Z [2,3,4]. The SVM method is used with different data, Korean characters known as Hangul.

Hangul recognition is more difficult compared with Latin due to its complicated arrangement. Hangul is arranged from 2 dimensions (both left and right side), while Latin is arranged from left to the right [5].

A Research on Hangul recognition has ever been conducted, where the writer applies the Stochastic Relationship Modeling to the recognition process of Hangul syllable writing. The output of the research is Hangul syllable texts[6].

So far, the research on Hangul recognition is conducted with Hangul texts output. The current research will improve the image conversion of Hangul with Latin text output. The image of Hangul converted into Latin text can be used as a learning material on how to read Hangul.

OCR system, in general, is divided into three steps. They are preprocessing, feature extraction, and recognition. Pre-process includes three stages: binarization to change the grayscale image into black white; segmentation, which is processed through connected component labeling, to separate the input into individual word; and thinning to decrease some information pattern (thin Line) in order to be easily analyzed [7]. The research will employ algorithm Zhang Suen, which works faster than the other thinning algorithms[8].

The next step, after pre-process, is feature extraction. It has an important role on recognition process. It works through generating the basic component of the image called features[9]. The feature extraction used in the current research is chain code. The last process is recognition, using the SVM method with some kernels *(linear, polynomial, and radial basis function).*

2. METHODOLOGY

Generally, OCR system is divided into three main steps. They are preprocessing (binarization, segmentation, and thinning), feature extraction in which in this research uses chain code, and recognition by applying Support Vector Machine (SVM) method. Figure 1 shows the general process of Hangul recognition.

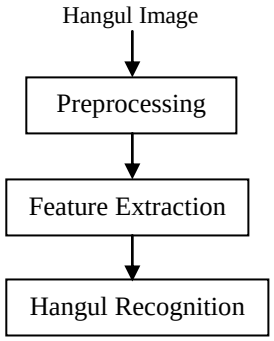

Figure 1. Block diagram of Hangul recognition

The input image used in the current research is the letter and Hangul word. The letter consists of 21 vowels and 13 consonants, shown in Figure 2 with Latin letter. Each letter has 15 different forms. The whole data are amounted to 510.

Figure 2. The Letters of Hangul and Latin[10]

Meanwhile for word, there are 6 ways on how to arrange the letter of Hangul into word. The first type is shown in Figure 3[10]. The discussion focuses on data type 2.

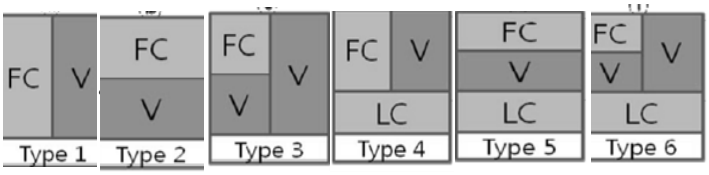

Figure 3. 6 the ways to arrange the letter of Hangul[10]

Meanwhile, the example of type 2 Hangul word is shown in Figure 4. Each word consists of 6 different forms. They are achieved by changing the word font. The used fonts are Arial, Batang, Dotum, Gaeul, Gulim, and Malgun Gothic.

	Training Data				Testing Data	Latin
보	보	보	보	보	보	Bo
뵤	뵤	뵤	뵤	뵤	뵤	BYO
부	부	부	부	부	부	BU
뷰	뷰	뷰	뷰	뷰	뷰	BYU
브	브	브	브	브	브	BEU
소	소	소	소	소	소	SO
쇼	쇼	쇼	쇼	쇼	쇼	SYO
수	수	수	수	수	수	SU
슈	슈	슈	슈	슈	슈	SYU
스	스	스	스	스	스	SEU

Figure 4. The example of Hangul word

2.1 Preprocessing

The preprocessing includes 3 steps. First, the binarization or thresholding, is implemented to change the grayscale image become black white. The process of thresholding will produce the binary image, the image which has two steps of grayish (black and white). Generally, the process of floating the grayscale image to produce the biner image are as follows[11]:

$$g(x,y) = \begin{cases} 1 \; if \; f(x,y) \geq T \\ 0 \; if \; f(x,y) < T \end{cases} \quad (1)$$

With g (x,y) is the binary image from grayscale image f (x,y) and T assert the percentage of threshold.

Second, thinning is used to decrease some information to a pattern becomes thin line in order to be easy to analyzed[7]. In this case, it will be applied the Zhang Suen algorithm which has faster performance compare with the other thinning algorithm[8]. To process thinning algorithm is shown in the Figure 6. This algorithm uses the pixel 3x3 and 8 degrees as in the Figure 5. P1 is a pixel that will be checked, if it fulfills the fixed condition, so the pixel will be deleted. The conditions are as follows[12]:

(a) $2 \leq B(P_1) \leq 6$ (2)

(b) $A(P_1) = 1$ (3)

(c) $P_2 \times P_4 \times P_6 = 0$, and (4)

(d) $P_4 \times P_6 \times P_8 = 0$ (5)

(e) $P_2 \times P_4 \times P_8 = 0$, and (6)

(f) $P_2 \times P_6 \times P_8 = 0$ (7)

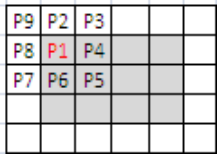

Figure 5. The pixel 3x3 with 8 degrees

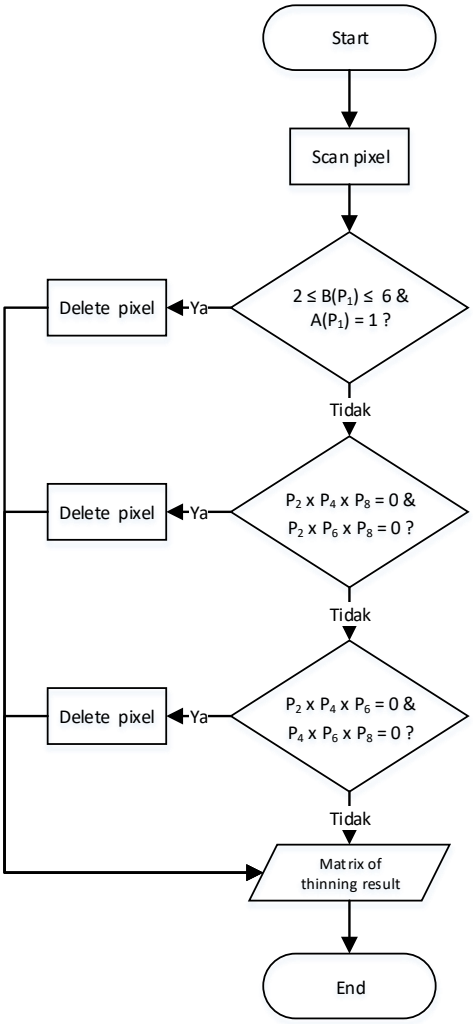

Figure 6. The Diagram algorithm of Zhang Suen

2.2 Feature Extraction

The next step after preprocessing is feature extraction, which has an important role on recognition. This process will generate the necessary component of an image called features[9]. The used feature extraction is chain code which functions as the direction search. The direction usually uses the following regulation Figure 7.

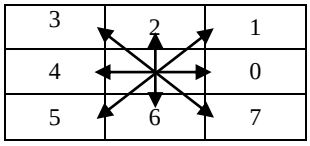

Figure 7. The direction of sequence code with 8 degrees[13]

The sequence code is made through checking the direction of a pixel connected to the other pixels with 8 degrees. Each direction has different number. The pointed sign shows the first pixel. It is a place where the next steps will be fixed[13]. Figure 8 shows letter B with its sequence code.

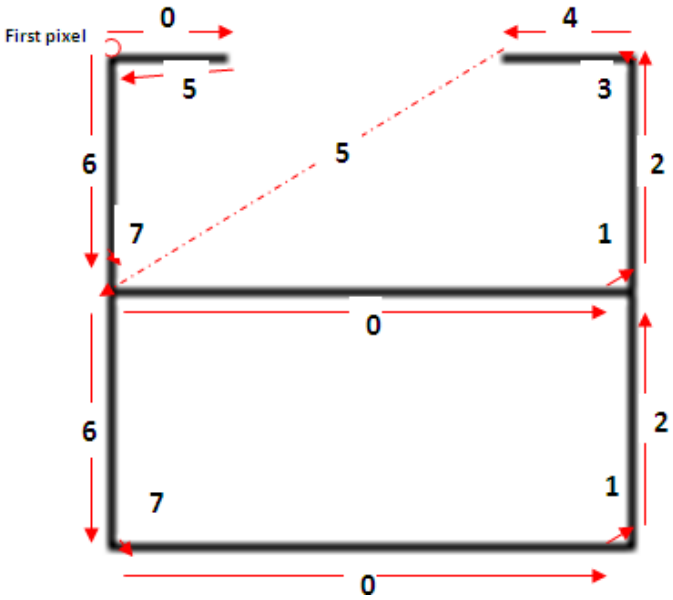

Figure 8. The direction of the sequence code in letter B

In order to be processed into SVM, the feature extraction must have the same amount of features. Therefore, normalization needs to be done. It also aims to decrease the amount of feature which reoccurs. The normalization process for chain code can be done with the following pattern[12]:

$$Fitur_n = \frac{F_n}{N_n} x\ N_{norm} \quad (8)$$

Note:
N = the amount of feature wanted
F_i = the amount of feature normalized
$\sum F_i$ = the amount of all letters normalized

2.3 Support Vector Machine (SVM)

The Support Vector Machine (SVM) is found in 1992 by Boser, Guyon, and Vapnik. The basic concept is the combination of computation theories introduced in previous years, such as the margin hyperplane and kernel. The concept of SVM can be seen as an effort to look for the best hyperplane to separate two classes in the input grade.

Figure 9 shows some data of the two class member (+1 and -1), where (a) shows some alternative separated line (Discrimination Boundaries), and (b) shows the best hyperplane. The best hyperplane can be found by measuring the distance between the hyperplane and the nearer data known as margin [13]. The data in the margin is called support vector[14].

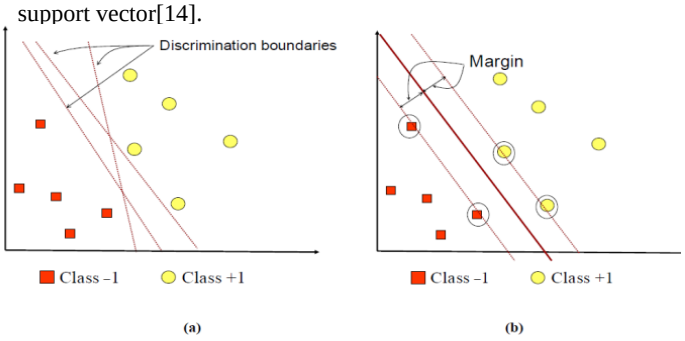

Figure 9. (a) The alternative separated field, (b) The best separated field with the biggest margin[14]

Practically, the real data does not only consist of two classes and they cannot be separated linearly. To solve this, an approach needs to be conducted so that SVM is able to classify the data input with N-Dimension or multi class, one of which is one against one[14]. Besides, to arrange the data input into higher dimension feature space, a function called kernel is needed. Table 1 shows some kernels used in SVM [15], and Figure 10 shows the process of recognition with SVM.

Table 1. Kernel function in SVM[16]

Kernel	Fungsi
Linear	$K(x,y) = x,y$
Polynomial	$K(x,y) = (\gamma x.y+r)^d$
Radial Basis Function	$K(x,y) = \exp(-\gamma\|x-y\|^2, \gamma>0$

Υ, r, and *d* are kernel parameter

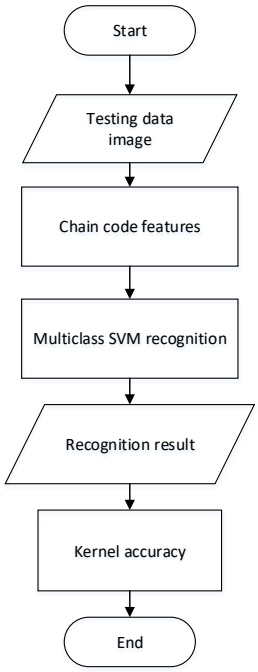

Figure 10. The diagram of Hangul recognition line with Multiclass Support Vector Machine

3. EXPERIMENT RESULT

Algorithm line Zhang Suen in Figure 6 shows that slight result is produced such as in Figure 11 (b).

(a) (b)

Figure 11. (a) Binary image, (b) Letter CH after thinning

After achieving the slight feature, the system takes it in accordance with the direction search in Figure 7. It generates the features of CH letter as follow:
0;0;0;0;0;0;0;0;0;0;5;6;6;6;6;6;6;6;6;6;6;6;6;6;6;6;6;5;4;4;
4;4;4;4;4;4;4;4;4;4;4;4;4;4;4;4;4;4;4;4;4;4;4;4;4;0;0;0;0;0;0;
0;0;0;0;0;0;0;0;0;0;0;0;0;0;0;0;0;0;0;0;0;0;0;0;0;5;6;6;6;6;6;
6;6;6;6;6;6;6;6;6;6;6;6;5;. . . ;CH;

If the feature is normalized according to the pattern (8), it has the same amount as the minimal feature from input image. Then, it will generate the following normalization feature:
0;0;0;0;0;0;0;5;6;6;6;6;6;6;6;6;6;6;6;6;5;4;4;4;4;4;4;4;4;
4;4;4;4;4;4;4;4;4;4;4;0;0;0;0;0;0;0;0;0;0;0;0;0;0;0;0;0;0;
0;0;0;0;5;6;6;6;6;6;6;6;6;6;6;6;6;6;5;. . . ;CH;

After getting the feature, system will do the recognition process. The letter recognition consists of 34 letters; each of them formulates 15 forms. So, they are 540 in total. The data scenario is shown in Table 2.

Table 2. Data scenario of Hangul letter recognition

Data Scenario	Training Data	Testing Data
DS1	170 (data A)	170 (data C)
DS2	340 (data A+B)	170 (data C)
DS3	510 (data A+B+C)	170 (data C)

Data testing process for DS1 and DS2 uses new data which have not been tested before while that for DS3 uses the tested ones.

Accuracy result of Hangul letter recognition for every kernel is shown in Table 3.

Table 3. Accuracy result of Hangul letter recognition

Kernel SVM	DS1	DS2	DS3
Linear	88,82%	94,11%	100%
Polynomial	89,41%	94,7%	100%
RBF	89,41%	94,7%	100%

Recognition mistake often occurs to the letter which has the same form, such as 우 (U) with 유(YU) or the other way around. Another letter which looks similar is 의(UI) with 위 (WI). The system output of Hangul letter is shown in Figure 12.

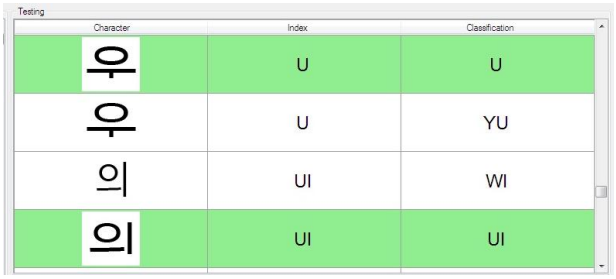

Figure 12. The result of Hangul letter recognition

In Hangul word recognition, researcher uses the form 2, where the training data are 195 and the testing data are 39. The accuracy for every kernel is shown in Table 4.

Table 4. Accuracy of Hangul word recognition

Kernel SVM	Accuracy
Linear	72%
Polynomial	72%
RBF	69%

Output from the recognition of Hangul word type 2 is shown in Figure 13. Recognition mistake occurs in the word which has almost similar form, such as 쵸 (CHYO) with 초 (CHO).

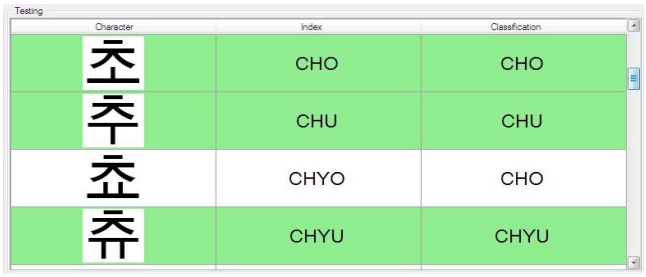

Figure 13. The recognition result of Hangul word type 2

4. CONCLUSIONS

The research concludes that the more the trained data, the higher the degree of accuracy. However, it needs to be reexamined until the fixed number of data which give the highest accuracy with SVM method is found.

In letter recognition process, kernel polynomial and RBF achieve the highest accuracy of 94,7% in data scenario 2 (DS2). On the other hand, linear process gives the lowest accuracy, 88,82%, in letter recognition, and RBF in Hangul word with 69%.

5. FUTURE WORK

The future research might employ the feature from the image with another method, while in the recognition process, the researcher can use SVM method with different kernel. Hangul recognition into Latin form may also be improved by adding the meaning of the trained word.

6. REFERENCES

[1] Seethalakshmi R., Sreeranjani T.R., & Balachandar T. 2005. Optical Character Recognition for Printed Tamil Text Using Unicode. Journal of Zhejiang University SCIENCE (2005), 1297-1305.

[2] Singh, D., Aamir Khan, M. & Bansal, A. 2015. An Application of SVM in Character Recognition with Chain Code. International Conference on Communication, Control and Intelligent Systems (CCIS). IEEE (2015), 167-171.

[3] Rajashekararadhya, S. V. & Ranjan, P. V. 2009. Support Vector Machine based Handwritten Numeral Recognition of Kannada Script. IEEE International Advance Computing Conference, 381-386.

[4] Tran, D. C., Franco, P. & Orgier, J.M. 2010. Accented Handwritten Character Recognition Using SVM – Application to French. IEEE International Conference on Frontiers in Handwriting Recognition, 65-71.

[5] Kyung-Won, K. & Jin H., Kim. 2003. Handwritten Hangul Character Recognition with Hierarchical Stochastic Character Representation. Proceedings of the Seventh International Conference on Document Analysis and Recognition.

[6] Kyung-Won, K. & Jin H., Kim. 2003. Handwritten Hangul Character Recognition with Hierarchical Stochastic Character Representation. IEEE Transactions On Pattern Analysis And Machine Intelligence, vol. 25, no. 9, 1185-1196.

[7] Lam, L., Seong-whan, L., & Suen, C. Y. 1992. Thinning Methodologies A Comprehensive Survey. IEEE Transactions on Pattern Analysis and Machine Intelligence, vol. 14, no. 9, 869-885.

[8] Haseena, M. H. F & Clara, A. R. 2017. A Review on an Efficient Iterative Thinning Algoritm. International Journal Research in Sciencee, Engineering and Technology, vol. 6, no. 11, 541-548.

[9] Nasien, D., Haron, H. & Yuhaniz, S. S. 2010. Support Vector Machine (SVM) For English Handwritten Character Recognation. IEEE Second International Conference on Computer Engineering and Applications, 249-252.

[10] Ju, S. & Shin, J. 2013. Cursive Style Korean Handwriting Synthesis based on Shape Analysis with Minimized Input Data. IEEE International Conference on High Performance Computing and Communications & International Conference on Embedded and Ubiquitous Computing, 2231-2236.

[11] Putra, D. 2010. Pengolahan Citra Digital. Yogyakarta: Penerbit Andi.

[12] Zhang, T. Y. & Suen, C. Y. 1984. A Fast Parallel Algorithm for Thinning Digital Patterns. Communication of the ACM, vol. 27, no. 3, 236-239.

[13] Sutoyo. Teori Pengolahan Citra Digital. Penerbit Andi. 2009.

[14] Vijaykumar, S. & Wu, S. 1999. Sequential Support Vector Classifier and Regression. SOCO'99. http://homepages.inf.ed.ac.uk.

[15] Chih-Wei H, Chih-Chung C, Chih-Jen L. A Practical Guide to Support Vector Machine. Department of Computer Science National Taiwan University, Taipei. May 2016.

[16] Fadel, S., Ghoniemy, S., Abdallah, M., Sorra, H. A., Shour, A., Ansary, A. 2016. Investigating the Effect of Different Kernel Functions on the Performance of SVM for Recocnizing Arabic Characters. International Journal Computer Science and Aplications, vol. 7, no. 1, 446-450.

International Journal of Computer Applications Technology and Research
Volume 7–Issue 07, 286-291, 2018, ISSN:-2319–8656

Combined Balanced Ternary Number System: An Approach to a New Computational Number System combining The Ternary Number System and the Balanced Ternary Number System in the field of Computational Mathematics

Md. Masudur Rahman
Noakhali Science and Technology University
Bangladesh

Md. Tanzil Mehadi Bappy
Noakhali Science and Technology University
Bangladesh

***Abstract*:**Logical systems are the core essence of our current computation system and these logics are based on binary number system. For the last few decades binary has been used as a core system. But in the upcoming future, it would require more efficient performance, high rate of computation and strong base in machine control system and artificial intelligence. So, the upgrade of computer number system is very necessary for more scope, speed, computation and analysis. The next step to move from binary is ternary (more precisely balanced ternary) and it is already used to develop a system several times. The implementable ternary number system in computer is the balanced ternary number system which was previously used to develop "SETUN". Actually, the balanced ternary number system is the binary implemented form of ternary using the system of overflow throughout the entire conversion. This is a continuous overflow system and overlaps the value every single time when the remainder is two (2). In order to overlap the value it is necessary to check if the remainder is 2 or not; this check increases the number of logical condition used during the conversion. Thus continuous overflow generally implies in complexity due to checking more logical conditions resulting in less efficient system performance. Considering this as a key point, the combined balanced ternary number system is developed which works with this overflow technique in order to increase the system performance. In the combined balanced ternary number system, the continuous remainder testing and overflow technique is replaced by partial overflow technique. In the partial overflow technique the overflow during conversion for any specific value is prohibited. In this number system overflow value is introduced with the remainder rather than the convertible value which results in less number of condition checking during the entire conversion process. As less logical condition is used, this new number system sharpens the performance of the conversion.

Keywords:Binary number system, Ternary number system, Balanced ternary number system, SETUN, Combined balanced ternary number system, Decoding complexity.

I. INTRODUCTION

For decades we have been using binary number system as the core computation number system. Binary is the core due to its own easy and established logical theorem and set of properties in Boolean algebra. Another key reason behind using binary is its simplicity in representation, computation, usability and analysis. It goes beyond saying that the feasibility of designing binary components played the most vital role for the development and stability of binary number system. But demand has changed since then and we need more advance technology, increased speed, performance and efficiency.

Earlier in the first decade of computer invention, it was really tough to build a binary based computer due to lack of technology and horrible sized components, let alone higher based computer. But over time these two main problems were overcome which resulted in highly improved and efficient technology with reduced size. Then for the first time in history, Soviet Union dreamt of something big and started an experimental approach with the invention of first three based computer named "Setun". They found that the ternary system (base 3) was really complex to implement then. So, they went to the alternative way [6] to implement ternary and that was balanced ternary [7]. Later some actions were taken to invent a full-fill ternary based computer which is very shortly known. Now in the age of nanotechnology and top level electronics, there's a possibility of designing complete higher base computer than the binary computer and the first stepping stone is ternary.The design and implementation of ternary circuitry were reported in [11]-[12]. A new type of transmission functions theory was reported in [14]. Here, the author has suggested that this theory can explain all the CMOS ternary circuits.

Though the first step is to be made in ternary, the system is going to be unveiled through balanced ternary [1]. Ternary, more precisely balanced ternary is more suitable for improved and advance computing is suggested by author in [9]. The reason behind using the balanced ternary (though it is a nonstandard positional number system) is the unavailability of implementable standard ternary logics [2] whereas balanced ternary uses the advanced Boolean theorem developed from binary system. Also it was quite strenuous to represent ternary directly in computer due to technological bindings. Balanced ternary was far much easier [3] to implement rather than ternary and the prime cachet was the uniformity of digits in balanced ternary (-1, 1, 0) respecting binary (0, 1). But the ultimate factor that energized to give priority to balanced ternary over ternary was its overflow method which resulted in a more forcible way with less complexity [5] and this overflow is the most crucial issue on the article. And in some cases it would be crucial also on cryptosystem [4]. Another fact is that Rotation Symmetric Boolean function has beckoned the interest of theoretician as well as practitioners in the field of cryptography [8] [10].

As mentioned earlier, the balanced ternary number system includes continuous overflow process which makes it effective to implement but results in a large number of logic checking. The combined balanced ternary is developed hereby to deal with this extra number of logic checking and continuous overflow.

II. MATERIAL AND METHOD

In this section, we describe the used techniques in computation (eg. Binary number system, balanced ternary number system) and the newly proposed combined balanced ternary number system. We have also put a comparison of some basic values of the number systems in tabular form.

In the early days of computing, a few experimental Soviet computers were built with balanced ternary instead of binary, the most famous being the Setun, built by Nikolay Brusentsov and Sergei Sobolev. The notation has a number of computational advantages over regular binary. Particularly, the plus-minus consistency cuts down the carry rate in multi-digit multiplication, and the rounding-truncation equivalence cuts down the carry rate in rounding on fractions. Balanced ternary also has a number of computational advantages over traditional ternary. And the new system that is developed on current time named "The Combined Balanced Ternary" is likely to replace the balanced ternary with more efficiency in performance.

A. Existed Number Systems Analysis in Computation Scenario:

There are numerous number systems. Yet we use the easiest possible number system with lower base for computation which gives us the advantage to do calculation in easier but long process. The basic number systems are Decimal, Binary, Octal, Hexadecimal etc. Among all the number systems, Binary is the simplest though it's not optimal. The optimal number system is "e" based. The nearest number system to optimal value is ternary number system that's why it is much significant.

Smaller the base, higher the bits to represent a value; this is the basic theory in computation. Still binary is used to develop computer system due to the simplicity and availability of theorems based on it. But when it comes in terms to ternary, we can't implement it in direct basis. Instead, we implement it in the nonstandard balanced ternary process which is closely connected to binary. Again we can't use high level based systems in large manner due to high electronics complexity. But, as it is important to upgrade the number system which is capable to provide better performance, the system should be initiated with the complete implementation of ternary number system. The proposed system below can be the initial step to do so.

Currently balanced ternary number system is used as the core to represent the ternary number system on the way to its implementation in computer system. But a major fact is that it is unable to represent the actual ternary number system. Perhaps, it is a binary converted form of ternary with continuous overflow technique. So, if we move towards the ternary representation, the first approach would be to deal with this continuous overflow technique. On the work we are focused with this fact.

1. Traditional Ternary Number System:

In traditional ternary the base value is 3 and the used digits are 0, 1 and 2. In digital system this two is currently unavailable to represent in direct independent bit form due to the binary logic properties of electronics. Let's take a look to a small conversion-

$(17)_{10} = (\ldots?\ldots)_3$

Now, 3/17

3/5-2

3/1-2

So, the conversion is: $(17)_{10} = (122)_3$

Reversely, $(122)_3 = 1*3^2+2*3^1+2*3^0$

$= 9+6+1$

$= 17$

2. Balanced Ternary Number System:

Balanced ternary number system is a nonstandard ternary representation form in binary properties. For a system it is found that the highest value is supposed to be 1 less than the base. But in balanced ternary, we can use a different system in conversion from any other type. Here we can introduce the 'overlap' technique. We jump on the next number if the remainder is only equal to 2. And for that overlapping we will write the " -1" in the place of remainder. Its advantage over the traditional ternary number system is that it is representable through binary system though it uses continuous overflow. Let's check a conversion-

3/17

3/6-(-1)

3/2-0

3/1-(-1)

So, now the reverse conversion is:

$(17)_{10} = (1(-1)0(-1))_3$

$=1*3^3+ (-1)*3^2+0*3^1+ (-1)*3^0$

$= 27+ (-9) + 0+(-1)$

$= 27-10$

$= 17$

B. Proposed System (Combined balanced ternary):

In this section we are going to describe our proposed number system technique. Firstly, we would like to mention that the basic theme of this proposed system is influenced by the combination of balanced ternary and raw ternary, that's why we named it combined balanced ternary. Like the balanced ternary, it is a nonstandard number system but the proposed system differs from the balanced ternary in the sense of continuous overflow; in terms it uses a new method named partial overflow.

When it comes to continuous overflow, the value is randomly checked with its default criteria if overflow is possible or not. A worth mentioning factor about continuous overflow technique is that it is firstly checked through the remainder value and then executed on the root value.This lags the system through logical execution. Because the repeat of the overflow logic check in every times as well as new execution (more precisely computation) on the root value cost times which results in low performance.

If this repeat process of overflow possibility checking can be reduced then we are optimistic of getting better performance

On the contrary, the proposed system is based in partial overflow technique. In partial overflow, the overflow possibility is checked through the remainder but no extra computation is done over the root value, instead it deals with the remainder with the default value that is predetermined. This predetermined default value enables less logical execution than the continuous overflow technique.

1. Predetermination of default value for partial overflow:

The main problem we face in implementing ternary is due to its 3rd value "2." To represent this "2", balanced ternary was developed. This value is responsible for the continuous overflow technique. So, if we want to do partial overflow technique, we need to deal with this value. The only overflow we will use in our partial overflow technique is associated with this value "2." Let's take overflow for 2-

bar as only 1 value is elapsed. Thus the positional value of "P" would be 3^{n+1} which is similar to the last value "1" under the bar. This relationship can also be stated as that the positional value of the digit next to the bar would be equal to the adjacent bar digit. On the example "P" and 1 (adjacent digit of bar) would have the same positional value. This would be the same for all similar situation.

4. Final conversion:

In, this section, we will show the execution of the proposed system. For this, we will take any random number for applying our technique. Let take 33. Now, we will convert this value in our proposed "Combined balanced ternary number system" and the will reverse it back to the decimal value.

$(33)_{10}$ = (..?...)

3/2 = 1(-1)

So, $(2)_{10} = (1(-1))_3$

Now reversely, $1*3^1 + (-1)*3^0 = 3-1 = 2$. Thus the overflow balanced ternary value for 2 is 1(-1). But in our partial overflow technique we will represent 2 by $\overline{\mathbf{1(-1)}}$ instead of 1(-1). The bar over 1(-1) means the entire digits under the bar would be represented as one digit.

2. Substitution between remainder and overflow value:

Substitution between the remainder and pre-determined value is a pivotal factor in our partial overflow technique. During ternary conversion, we will use no overflow in the system. Instead of continuous overflow we will only substitute bits.

The substitution will be done with the remainder only when the remainder becomes "2." If the remainder is "2" it will be replaced by the pre-determined default value $\overline{\mathbf{1(-1)}}$. This substitution keeps the root value free from continuous overflow in conversion.

3. Positional value assigning during reversing:

As we used $\overline{\mathbf{1(-1)}}$ instead of 1(-1) and the entire digits under the bar appeared to be a single digit, we need to make a change in assigning the positional value. In any sequence that contain $\overline{\mathbf{1(-1)}}$, the right (-1) under the bar would follow the sequence of positional power and so as the next 1. But when the computation will complete the bar it would count as only one positional power has elapsed. Let's consider a case for better understanding-

Suppose, "P$\overline{\mathbf{1(-1)}}$Q" is a sequence which need to be reversed. Now, let's consider the positional power of "Q" is 3^{n-1} then the positional power of (-1) under the bar would be 3^n, and for 1 under the bar it would be 3^{n+1}. But when the process will be executed right after the bar, it will calculate the whole

3/33
3/11-0
3/3-2 = [3-($\overline{\mathbf{1(-1)}}$)]
3/1-0

So, the converted value in combined balanced ternary would be, $[10\ \overline{\mathbf{1(-1)}}\ 0]_3$.

Reversely, $[10\ \overline{\mathbf{1(-1)}}\ 0]_3 = 1*3^3+0*3^2+1*3^2+ (-1)*3^1+0*3^0$
$= 27+0+9-3+0 = 33$

Thus, $(33)_{10} = [10\ \overline{\mathbf{1(-1)}}\ 0]_3$

This conversion process is true for any value "n."

5. Algorithm and flowchart:

Algorithm for "Combined balanced ternary" conversion from decimal value is given below-

Step 1. Initialize the value (X) to be converted in ternary and select P= 3.

Step 2. Do steps 3 to 5 when X ≥ 3.

Step 3. Divide X by P and keep the remainder (R) sequentially.

Step 4. If R= 2 go to step 5, else continue.

Step 5. Replace R by $\overline{\mathbf{1}(-\mathbf{1})}$ and keep sequentially.

Step 6. If X = 2 go to step 7 else keep the value as remainder.

Step 7. Replace X by $\overline{\mathbf{1}(-\mathbf{1})}$ and keep sequentially.

Step 8. Stop.

The flowchart is given below-

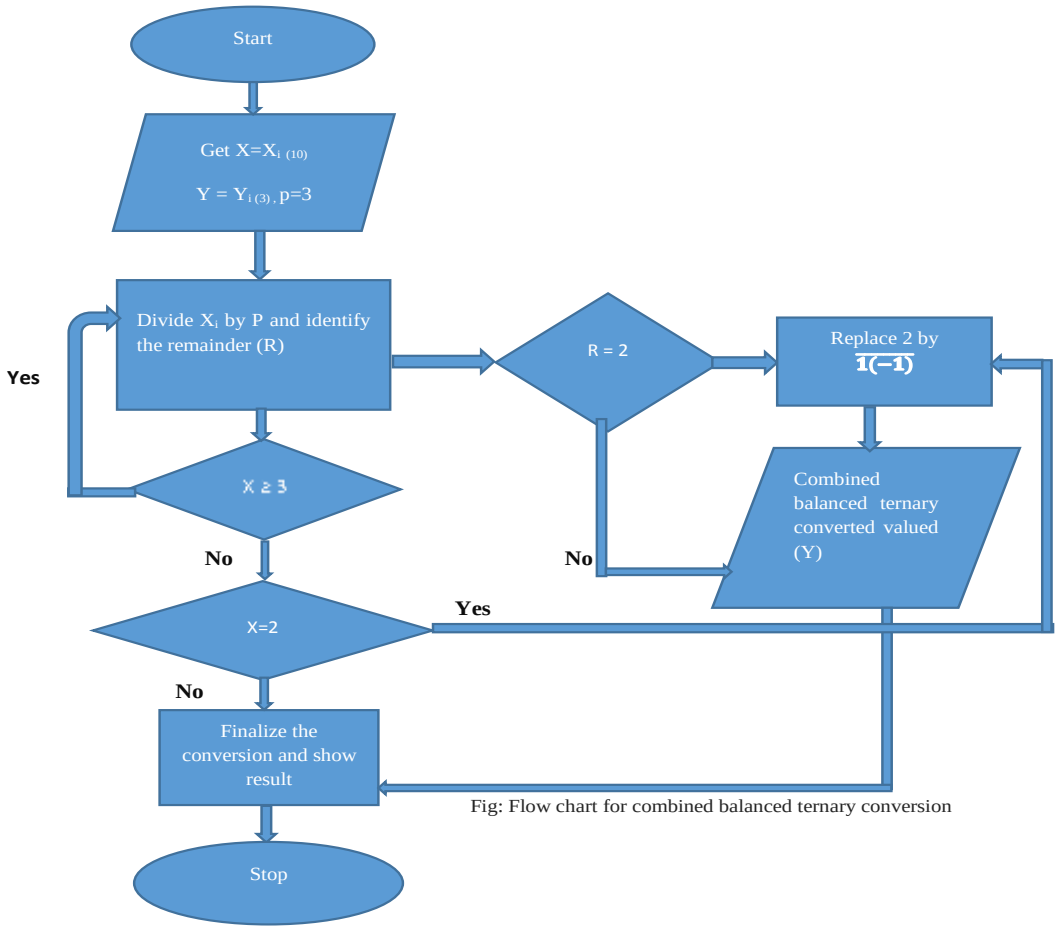

Fig: Flow chart for combined balanced ternary conversion

III. RESULT AND DISCUSSION

In this section we will discuss about the outcome from the proposed number system and its potentiality to the computation. The primary goal of this work was to develop a system that would be more precise to ternary system than the balanced ternary system.

A. Outcomes:

Thecombined balanced ternary number system can be said as the sister number system of both balanced ternary and ternary. It has a completely new technique of ternary conversion. The core outcomes of the proposed system are as follows-

1. Creation of a new number system:

Binary number system is the core number system of computer currently. Ternary number system is the future but it isn't implementable directly thus balanced ternary is developed. ON the sequence, the combined balanced ternary is another addition as an implementable ternary number system form through binary. This number system is unique in its own technique. And, of course it's worth mentioning that the partial over flow technique used in the system is totally new in the era of mathematics and

number system. This technique will open some new ways to rebuild or reshape any systems through allowing to think in a different manner with the number systems. A major factor is that it will insist to consider the existed number system to be reconstructed and there may rise some new potentiality with the rebuilt systems.

2. Lessening the complexity of the balanced ternary:

The basic goal of this new number system is to reduce the complexity of the implementation of balanced ternary though it is in the initial development process. The newly developed combined balanced ternary number system is expected to replace the balanced ternary number system over time due to some potential computational mathematical properties such as-

*Firstly,*less use of logic than the balanced ternary number system. Still it works explicitly like the balanced ternary.

*Secondly,*it is expected to provide all the past benefits of balanced ternary number system though it requires complete development of the system.

3. Increase the speed of computation:

Another prime outcome of this proposed system is to achieve higher rate of throughput in the computation work. And this can be simply achieved through using the newly introduced number system as the processor (Yet to develop any) of this number system would be simpler than the processor of balanced ternary due to lessening the number of logic that was needed to be executed in the previous system.

B. Comparative value table:

Among all the number systems, four number systems are most widely used. They are Decimal, Octal, Hexadecimal and Binary. As we are intended to discuss about ternary, we have given a value table that includes the comparative value between the systems as well as including the Balanced ternary and proposed Combined balanced ternary system.Here is a combined ternary value table comparing to other systems:

Decimal	Hexadecimal	Octal	Binary	Ternary	Balanced Ternary	Combined Balanced Ternary
0	0	0	0	0	0	0
1	1	1	1	1	1	1
2	2	2	10	2	1(-1)	$\overline{1(-1)}$
3	3	3	11	10	10	10
4	4	4	100	11	11	11
5	5	5	101	12	1(-1)(-1)	$1\overline{1(-1)}$
6	6	6	110	20	1(-1)0	$\overline{1(-1)}0$
7	7	7	111	21	1(-1)1	$\overline{1(-1)}1$
8	8	10	1000	22	10(-1)	$\overline{1(-1)1(-1)}$
9	9	11	1001	100	100	100
10	A	12	1010	101	101	101
11	B	13	1011	102	11(-1)	$10\overline{1(-1)}$
12	C	14	1100	110	110	110
13	D	15	1101	111	111	111
14	E	16	1110	112	1(-1)(-1)(-1)	$11\overline{1(-1)}$
15	F	17	1111	120	1(-1)(-1)0	$1\overline{1(-1)}0$

*C. Limitations:*Nothing is free of limitation. There's a few limitations in newly developed combined balanced ternary though it is in the initial development process. The major limitations are stated below:

*i.*The main limitation of the system is its decoding complexity due to its totally new concept of positional value.

*ii.*Another key limitation is that it requires higher number of memory space than the previously used systems in some cases.

IV. CONCLUSIONS

It is beyond saying that the ternary number system is the upcoming future of computational mathematics. Though it is expected that the balanced ternary system will rule in ternary computing, the newly introduced combined balanced ternary system would be a strong contender to balanced ternary in implementation if the new system is developed properly with full characteristics.

The development of the combined balanced ternary is currently on its initial process. There's still a lot things to do in order to develop a complete combined balanced ternary number system for implementation purpose. Once the system is developed and it is in its full form then it could be an epoch making move in the era of computation sector.

REFERENCES

1. Third Base by Brian Hayes, American scientist, Vol. 89, No.6, 2001, pp. 490-494.

2. A New Moduli Set for Residue Number System in Ternary Valued Logic by M. Hosseinzadeh and K. Navi.[Research paper published on Science Alert].

3. Constructions of balanced ternary designs by D. G. Sarvate [Cambridge University Press,Journal of the Australian Mathematical Society]

4. J. Adikari, V. S. Dimitrov, L. Imbert, Hybrid Binary-Ternary Number System for Elliptic Curve Crypto System, IEEE Transactions on Computers, Vol-60, No.-2, Feb-2011.

5. Towards a balanced ternary FPGA by Paul Beckett Electrical & Computer Engineering, RMIT University, Latrobe St., Melbourne, Australia.

6. : D. Donovan, 'Methods for constructing balanced ternary designs',Ars Combin. 26A, to appear.

7. A. Francel, Margaret & Hurd, Spencer. (2008). Nested balanced ternary designs and Bhaskar Rao designs. The Australasian Journal of Combinatorics [electronic only].

8. P Stanica and S Maitra, Rotation Symmetric Boolean Functions-Count and Cryptographic Properties, Discrete Applied Mathematics,Vol-156,n0.-10,May 2008.

9. Balanced- Ternary Logic for Improved and Advanced Computing by Shamshad Ahmad, Mansaf Alam Deptt. Computer Science, JMI, New Delhi 10.

10. 10. P. Sarkar, S. Maitra, Constructions of Nonlinear Boolean Functions with Important Cryptographic Properties. In Advances is Cryptology-EUROCRYPT 2000,pp 485-506,Springer Verlog, 2000.

11. A, Srivastava, K Venkatapathy," Design and implementation of a low power ternary full adder", VLSI Design,1996,VOl-4, No.-1,pp 75-81

12. A.Sathish Kumar, A. Swetha Priya, The Minimization of Ternary Combinational Circuits -A Survey,A. Sathish Kumar et.al./International Journal of Engineering and Technology,Vol2(8),2010,pp 35376-3589,ISSN 0975-5462.

13. A.P.Dhande, V.T. Ingole, Design and Implementation of 2 Bit ternary ALU Slice, Third International Conference; SETIT 2005-Tunisia.

14. X.W.Wu, CMOS Ternary Logic Circuits, IEEE Proceedings, Vol 137, Pt.G, No. 1, Feb 199